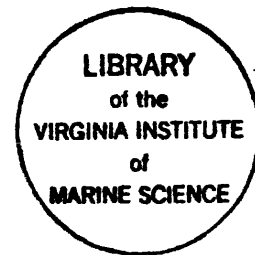


RESPONSE ¹⁰ ~~OF~~ FRESHWATER INFLOW IN
THE RAPPAHANNOCK ESTUARY, VIRGINIA
- OPERATION HIFLO '78 -



JULY 1981
CRC PUBLICATION NO. 95

RESPONSE TO FRESHWATER INFLOW IN THE RAPPAHANNOCK ESTUARY, VIRGINIA
OPERATION HIFLO '78*

by

Maynard M. Nichols
College of William and Mary
Virginia Institute of Marine Science
Gloucester Point, Va. 23062

L. Eugene Cronin
Chesapeake Research Consortium, Inc.
Annapolis, Md. 21403

William B. Cronin
The Johns Hopkins University
Chesapeake Bay Institute
Shady Side, Md. 20867

M. Grant Gross
National Science Foundation
Washington, D.C. 20550

Bruce W. Nelson
University of Virginia
Charlottesville, Va. 22904

Jack W. Pierce
Smithsonian Institution
Washington, D.C. 20560

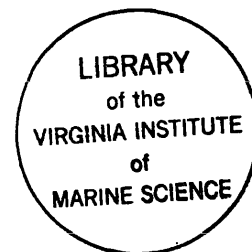
Robert E. Ulanowicz
University of Maryland
Chesapeake Biological Laboratory
Solomons, Md. 20688

CRC PUBLICATION NO. 95

CHESAPEAKE RESEARCH CONSORTIUM, INC.

May, 1981

*A complementary volume, Data Report, Operation HIFLO '78, is
available from the Chesapeake Research Consortium. (CRC Publ. No. 99)



ABSTRACT

The HIFLO experiment was organized by the Chesapeake Research Consortium to develop techniques for a coordinated response to emergencies and major environmental events. The purpose of the experiment was to learn how the Rappahannock Estuary, Virginia, responds to high river inflow and influx of sediment. Synoptic measurements of flow, salinity and suspended sediment were obtained at slack water along the 144 km estuary between March 28-April 1, 1978. Flow and sediment loads were monitored for nearly one month at four key points in the estuary and the watershed.

The HIFLO event of March 25-29, 1978, discharged up to 358 m^3 per second, an inflow that occurs once every year on the average. During four days, 21,000 tons of sediment, about 30 percent of the annual average river input, was supplied to the estuary head.

The storm triggered a sequence of dynamic events: (1) initial response, (2) shock, (3) rebound, and (4) recovery. The storm sediment load moved downstream 60 km and temporarily deposited during late stages of high river inflow. Seaward transport was limited by rapid settling of relatively coarse flood-borne particles and by the sediment influx lagging the river inflow. The HIFLO observations suggest that transport through freshwater reaches is a stepwise process involving temporary accumulation followed by resuspension and downstream transport.

The indirect response to high river inflow consisted of freshening the salt intrusion and changing hydrodynamic conditions for transport at the inner limit of salty water. The high inflow displaced the inner limit of salty water seaward 13 km, shifted the current null zone seaward and increased stratification. These changes enhanced the trapping effectiveness of the estuarine circulation system and intensified the turbidity maximum. Sediment loads returned to pre-storm levels within five days while net flow and salinity recovered within 16 days. The results provide new information for improving our understanding of estuarine dynamics and for addressing future problems of water quality and inflow modifications.

CONTENTS

	Page
1. INTRODUCTION	1
2. SITE CHARACTERISTICS	6
3. FIELD METHODS AND LABORATORY TECHNIQUES	7
4. RESULTS	12
Storm and Runoff	12
Tide Effects	17
Salinity Response	17
Flow Response	19
Suspended Sediment Response	25
Response Sequence	28
Particle Size	30
Particle Composition	31
5. SUMMARY	37
6. COMMENTARY	38
7. ACKNOWLEDGEMENTS	39
8. REFERENCES	41
APPENDIX 1, 2	43
APPENDIX 3	44
APPENDIX 4	45
APPENDIX 5	46

1. INTRODUCTION

More sediment, nutrients and pollutants are discharged into an estuary during a few days of flood inflow than during many months or years of average inflow (Meade, 1972; Schubel, 1977), but few observations document the sedimentary response of an estuary to high freshwater inflow. Such inflows are usually unexpected and estuarine water characteristics change too rapidly to permit systematic measurements. Moreover, the expenditure of effort and number of sampling vessels required on short notice is beyond the resources of a single research group or institute. Yet, freshwater inflow observations are a key to improving water quality; especially to ameliorate the effects of high turbidity, depleted oxygen and low salinity which can cause oyster mortalities (Zaborski and Haven, 1980). Many significant ecological effects are noted by Snedakar, et al., 1977. Exceptional sediment deposition shoals shipping channels, fills boat basins, and blankets oyster grounds. Suspended sediments adsorb toxic contaminants, nutrients and organic matter, and thus can affect plant production and the distribution of shellfish, plants and other life.

The HIFLO experiment was planned to observe and evaluate the response of an estuary to high freshwater inflow and high influx of suspended sediment. Of special interest are the questions: How far seaward does the sediment load from an event go before settling to the bed? How do the hydrodynamic conditions for sediment transport change? What is the sequence of estuarine processes triggered by a river flood?

Most estuarine observations are made during relatively stable conditions of average or low inflow; only a few observations record the effects of high inflow or floods under unstable flow regimes. Seaward displacement of circulation and salinity regimes is recorded by Rochford (1950) in Australian estuaries and by Inglis and Allen (1957) in the Thames, England. In some

estuaries, like the Gironde, France and Southwest Pass, Mississippi, floods push the salt intrusion and the turbidity maximum into or through the estuary mouth (Allen and Castaing, 1973; Meade, 1972). By contrast, most prior observations in the Chesapeake region, which were mainly taken after storm Agnes, 1972 (Nichols, 1977; Davis, 1977), showed that the salt intrusion was displaced far seaward but retained within the Bay. Sediment loads were largely deposited within upper reaches of the Bay or its tributaries. Storm Agnes observations in the Rappahannock were used to plan new observations for this study.

The observational approach was organized to meet three sub-objectives:

1. To measure the water and sediment discharge with time at key points along the river and estuary. These measurements were designed to record the river influx, or "stress", as well as the "response" in the estuary.
2. To observe synoptically the spatial distribution of selected hydrographic and sedimentologic parameters at a relatively short time scale, i.e. days.
3. To bring together scientific and operational resources of four Chesapeake Research Consortium institutions to undertake an important project which required diverse abilities and an assemblage of facilities.

To meet the first sub-objective, four key sites were selected for continuous monitoring of flow, current and sediment concentrations. Sites were located (Fig. 1) to take advantage of ongoing U.S. Geological Survey-Virginia State monitoring facilities at Remington and Fredericksburg in the drainage basin. Additionally, a sediment station was established on a pier of the FMC Corporation 1.6 km downstream of Fredericksburg and another on a bridge pier at Tappahannock. The Tappahannock station is located close to the average inner limit of salty water and in the zone of the turbidity maximum. A Beckman RQ-1 salinometer was installed on the bridge pier one meter above the bed. Current stations were located by VIMS in the channel axis 2.7 km seaward of the Tappahannock bridge and by CBI 1.8 km southeast of Windmill Point at the estuary mouth. These stations were occupied for about one month starting four to six days before peak flow at Fredericksburg. This

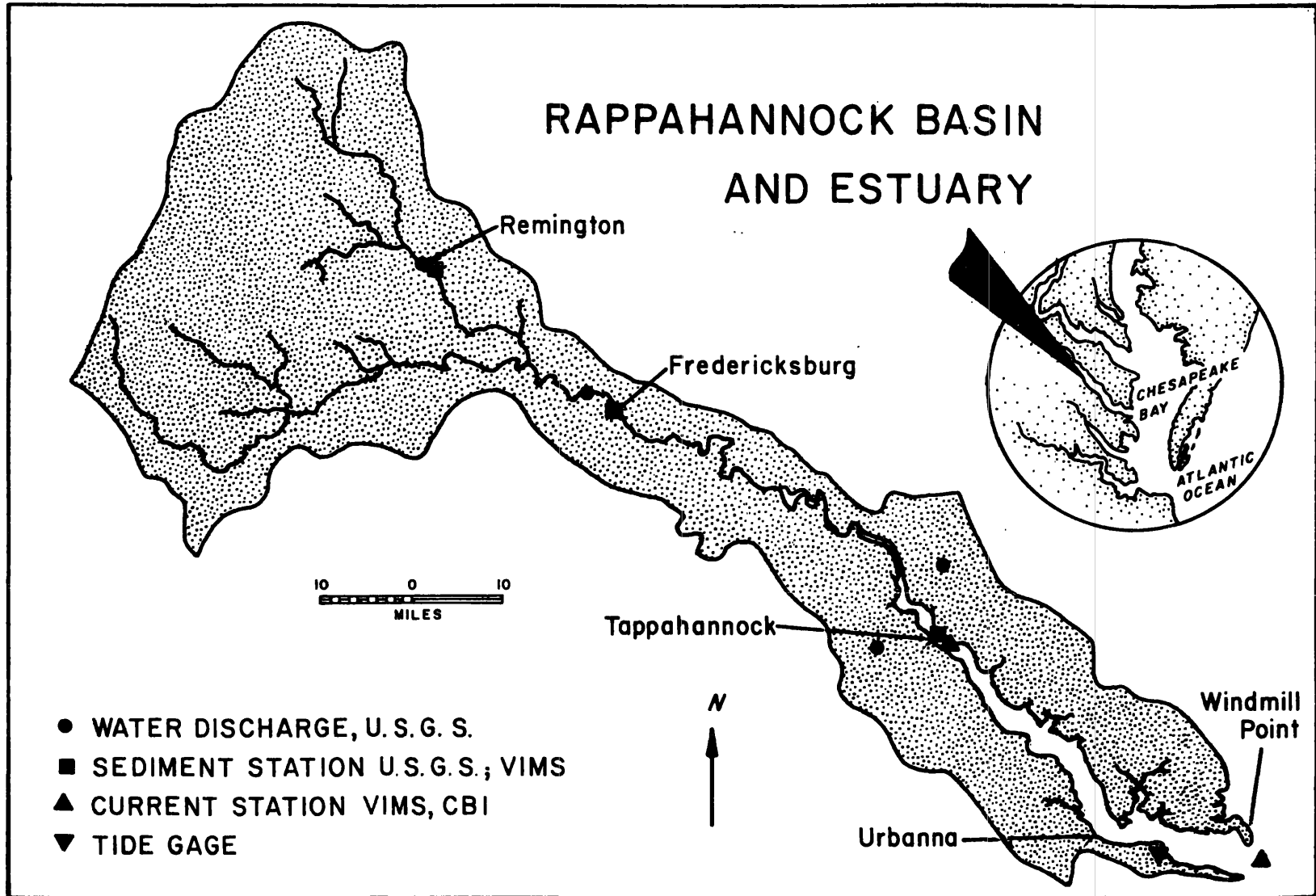


Figure 1. Location of the Rappahannock River basin and in relation to lower Chesapeake Bay, right. Location of water and sediment gaging stations at Remington, Fredericksburg, and Tappahannock as well as current metering stations near Tappahannock and Windmill Point.

observational period was selected because the history of flooding in the Rappahannock shows that the greatest frequency of floods occurs during this period.

To meet the second objective, field observations were planned to occupy stations at five mile intervals along the channel axis from the mouth to the fall-line at Fredericksburg, a distance of 147 km (92 miles), (Fig. 2). To compare data from station to station, observations were made at slack water, a time of minimal sediment resuspension from the bed. To observe changes associated with inflow, the longitudinal section was run every day for five days, March 28-April 1, after peak flow at Fredericksburg on March 27. For comparative data, a longitudinal section was run four days prior to, and again 14 days after, peak discharge, a time of recovery. Lateral variations were examined in a section across the estuary, R35, located near the salt intrusion head (Fig. 2). Distributions with depth in the sections were determined by either continuous vertical profiles, e.g. for turbidity, or water sampling, and in situ measurements at selected depth intervals. Field observations were supplemented and verified by one-day aerial observations from a light plane.

The third objective was met by a series of organizational meetings to plan and coordinate field logistics including vessel deployment. Transmissometers were intercalibrated by CBI, standard procedures developed and common recording forms selected. Following the field observations, data were reduced and analyzed either independently or jointly, and the results combined into the present report as well as a supplementary data summary. A critique of field operations was compiled and recommendations offered to the CRC Board of Trustees for responding to future events.

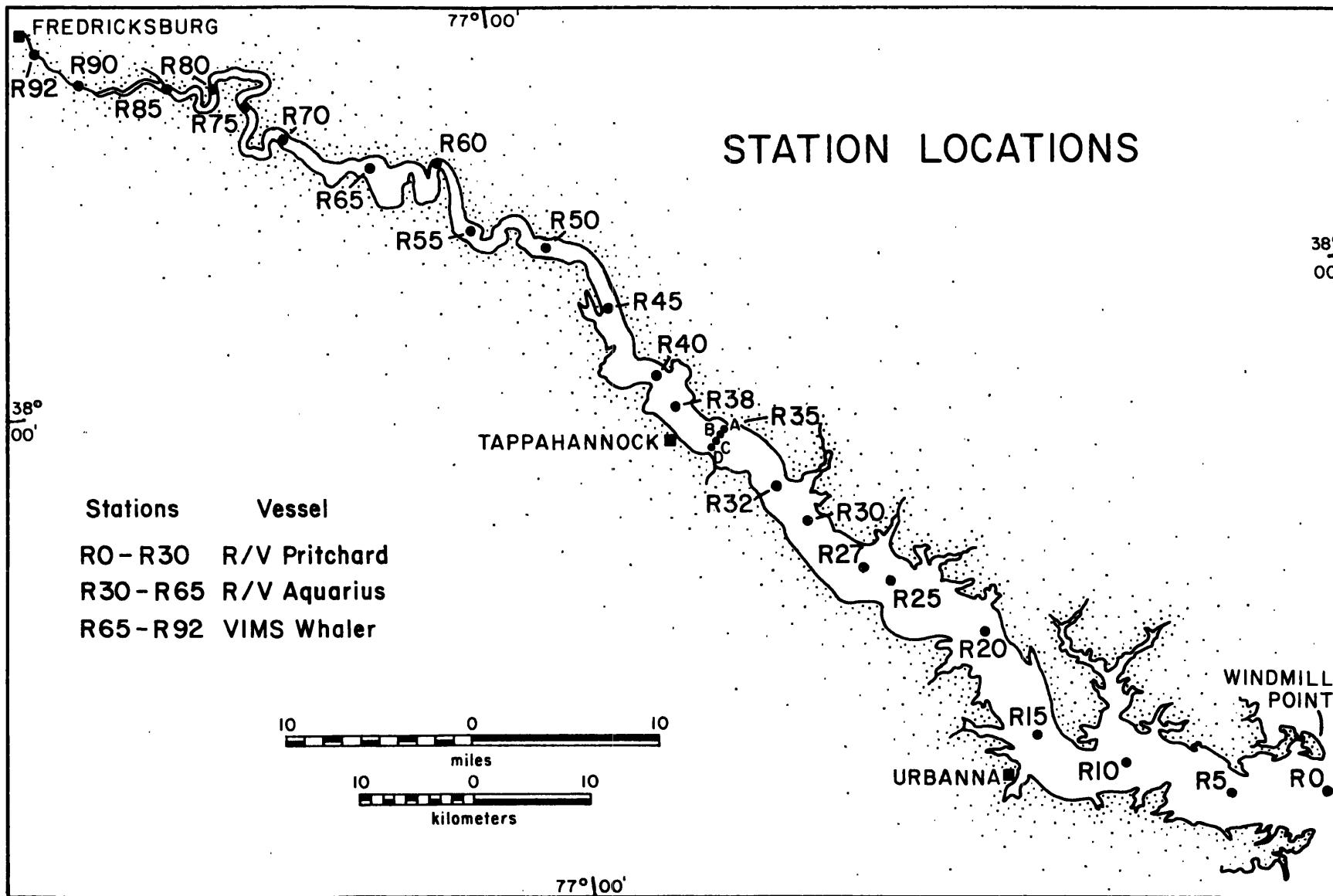


Figure 2. Station locations for longitudinal and lateral sections.

2. SITE CHARACTERISTICS

The Rappahannock was selected for study because it is of intermediate size; that is, large enough to produce high inflows and exhibit a response in the estuary. It is small enough to allow detailed observation within the limits of CRC resources. The estuary is relatively well known from prior studies (e.g. Ellison and Nichols, 1970; Huggett, 1974; Nelson, 1972; Nichols, 1977) and its river flow and sediment discharge are monitored at a number of points by the U.S. Geological Survey (Fig. 1). The runoff regime is short pulsed or "flashy" and partly predictable; it is not extensively modified by major dams or channel dredging. Pollution from point sources is largely controlled; but the banks and flood plains, which support agriculture, are potential non-point sources of nutrients and sediments. Other sediment sources include the banks, lateral tributaries, biological production in the estuary including shell and diatoms, the Chesapeake Bay via landward advection and erodible material from the estuary floor.

At average conditions of tide, i.e. 33 cm range at the mouth and 51 cm at Tappahannock (N.O.S., 1978), and average river inflow, i.e. $46.6 \text{ m}^3/\text{s}$ (1,646 cfs) at Fredericksburg (U.S.G.S., 1978), estuary water is partially-mixed. Fresh and salt water mix over a broad transition zone seaward of Tappahannock and stratification is relatively weak. These hydrodynamic characteristics are similar to those in other Chesapeake tributaries like the Potomac, York and Patuxent (Elliott, 1978; Ulanowicz and Flemer, 1978). Water movement follows a two-layered pattern with net seaward flow through the upper layer and net landward flow through the lower layer (Nichols and Poor, 1967). This circulation system determines the pathways for sediment transport in saline reaches. Freshwater reaches above Tappahannock are tidal up to Fredericksburg. Because this zone has a long form, transit time of water and sediment from the fall-line to the saline reaches is relatively long.

3. FIELD METHODS AND LABORATORY TECHNIQUES

Temperature, conductivity and salinity, optical transmissivity or turbidity, water depth, horizontal position, time, suspended solids (or sediment) concentration, particle size, particle microtexture and organic content were measured along longitudinal and lateral sections. Table 1 summarizes the variables, equipment used, and instrumental accuracy.

We measured temperature and conductivity from the R/V Pritchard, R/V Aquarius and R/V Whaler in situ using Interocean induction conductivity units, model 513, whereas on the R/V Blue Fox we used a portable Beckman Salinometer RS-5. The units were calibrated prior to deployment and recalibrated each day following CBI standard procedures.

We measured turbidity with in situ optical transmissometer sensors consisting of three CBI-type units with 5 and 10 cm path lengths and two Parteck units with 0.6 and 5 cm path lengths. Prior to deployment the units were intercalibrated in a single container using six different batches of muddy bed sediment collected from six sites along the estuary length. Figure 3A shows that optical response to different sediments of the same concentration varied within narrow limits $\pm 10\%$ for all samples except Fredericksburg. Final laboratory calibrations curves are given in Figure 3B.

We measured water depths with shipboard fathometers and sampling depths with a standard meter wheel. We obtained near-bottom water at 0.3 m off the bed using a van Dorn water bottle mounted in a tripod 0.3 m above its base. Time was read from shipboard clocks while horizontal positions were determined by radar and Loran C in the lower estuary, and dead-reckoning and bouy sightings in the upper estuary.

TABLE 1. Hydrographic and Sedimentologic Variables, Corresponding Measuring Equipment and Instrumental Accuracies.

<u>Variable</u>	<u>Equipment or Analysis & Accuracy</u>
Temperature	Interocean Induction Conductivity Unit, Model 513; $\pm 0.02^{\circ}\text{C}$ Beckman Salinometer, RS-5 $\pm 0.2^{\circ}\text{C}$.
Conductivity	Interocean Induction Conductivity Unit, Model 513; ± 0.02 millimohs. Beckman Salinometer, RS-5 ± 0.1 mh.
Optical Transmissivity (Turbidity)	Chesapeake Bay Institute, 5 & 10 cm. length; better than $\pm 2\%$ of range. Parteck, 5 & 0.6 cm Length; better than $\pm 3\%$ of range.
Water Depth	Meter Wheel and Shipboard Fathometers ± 0.3 m.
Suspended Sediment Concentration (solids)	Water samples processed by Millipore filtration; ± 1.0 mg/l.
Particle Size	Coulter Counter; $\pm 10\%$ in each size channel.
Particle Microtexture and Size	Scanning Electron Microscope and Micrographs.
Current Speed and Direction	Braincon Histogram current meters, Type 1381; speed, $\pm 3\%$ full scale; direction $\pm 5\%$.

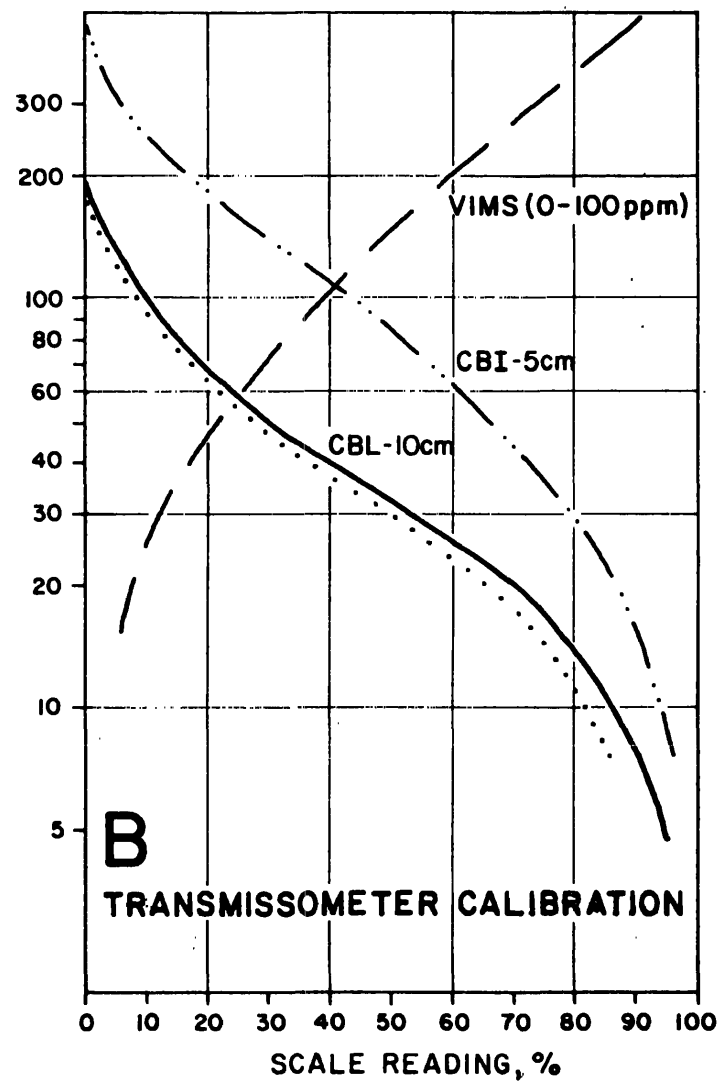
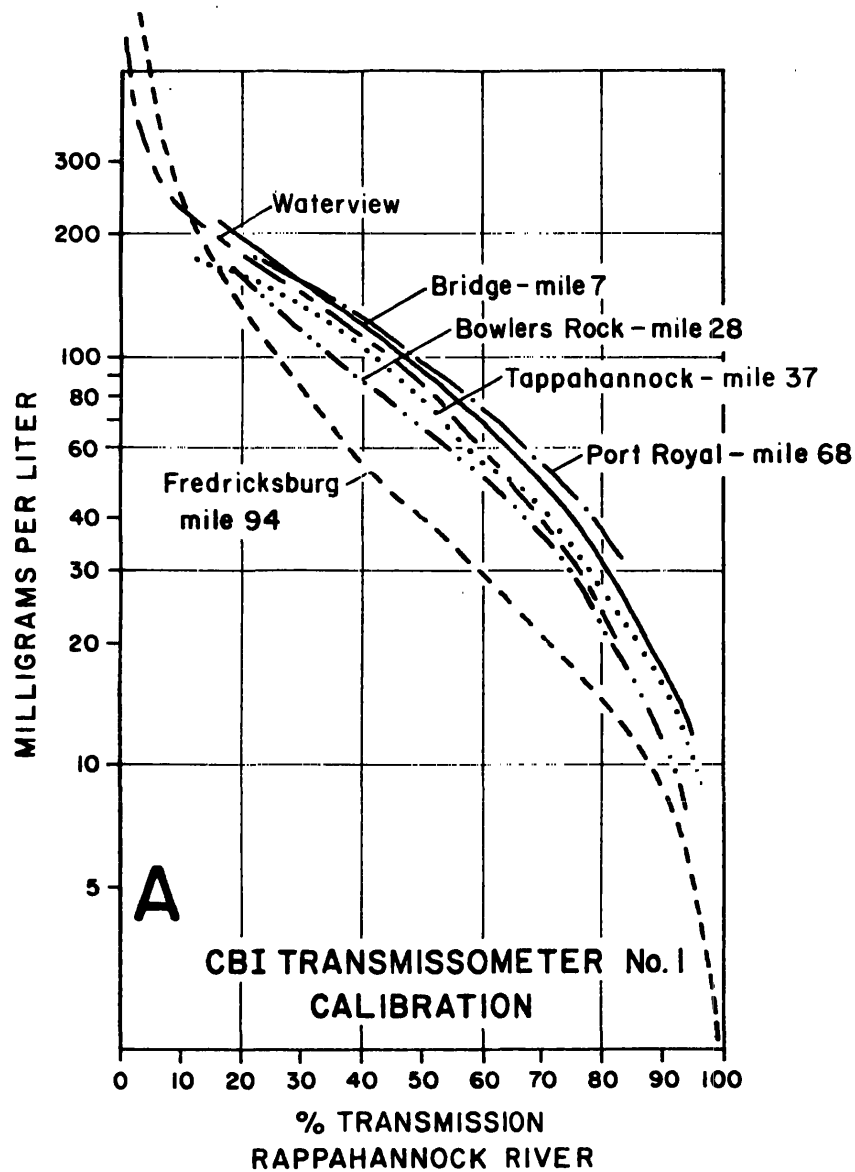


Figure 3. Transmissometer calibration curves:
 A. Optical response of CBI 5 cm unit to different samples of fine bed sediment from the estuary. B. Calibration curves for different transmissometer units used on Operation Hiflo.

The sampling protocol for longitudinal sections consisted of occupying stations along the channel axis at 5-mile intervals starting at the mouth. Sample and measurement depths between R0 and R60 were at 2-meter depth intervals through the water column and at 30 and 100 cm above the bed. Because upper reaches between R65-R92 are shallow, we sampled the depths: surface mid-depth, 30 and 100 cm above the bed. Similar depth intervals were sampled at four stations on the lateral transect, R35. We ran the longitudinal section close to slack water before flood, whereas we ran the lateral transect hourly for eight hours during flood and early ebb current. To cover the 92-mile length of estuary close to slack water, we assigned three vessels to different reaches: e.g. R0 to R30, R/V Pritchard; R30 to R65, R/V Aquarius; and VIMS Whaler, R65 to R92. We ran the longitudinal section six times and the lateral section eight times. We recorded observational data on hydrographic standard forms of the Chesapeake Bay Institute. Salinity was computed from conductivity data and in turn, the salinity and temperature data were used to calculate sigma-t (σ_t), a measure of water density using the relation:

$$\sigma_t = (\rho_t - 1)10^3$$

where ρ_t is the density at temperature t . Turbidity data were reduced to estimated sediment concentrations using the calibration curves for each unit (Fig. 3B), and particle size data were compiled into cumulative curves and histograms from which common statistical parameters were derived.

For total suspended sediment, or solids, we filtered a measured volume of fresh estuary water (50 to 200 ml) through a Millipore membrane filter of 0.80μ pore size. Laboratory processing mainly followed procedures of Strickland and Parsons (1972). For organic content, we determined the weight loss of selected filters after combustion at 1000°C for one hour.

We measured the particle size of suspended material, expressed as equivalent spherical diameters over the size range 0.6μ - 63μ with a Model TAI Coulter Counter. Samples were analyzed: (1) fresh aboard the R/V Aquarius within 2 hours after recovery; and (2) after storage for

three to five days and dispersion with 4% Calgon and agitation for 15 seconds. Additionally, we collected suspended material on Millipore filters on April 1 only for examination in a Scanning Electron Microscope. Between 1/2 and 2 ml of sample, depending on our estimate of concentration, was filtered through a 13-mm diameter, 0.47 μ m nominal pore size filter by means of low pressure. These filters were air-dried, vacuum coated with platinum-palladium, and micrograph images made at magnifications between 500X and 3000X using an SEM. From the micrographs, we identified microtextural types in different size classes larger than 0.5 μ m projected diameter and made corresponding frequency counts.

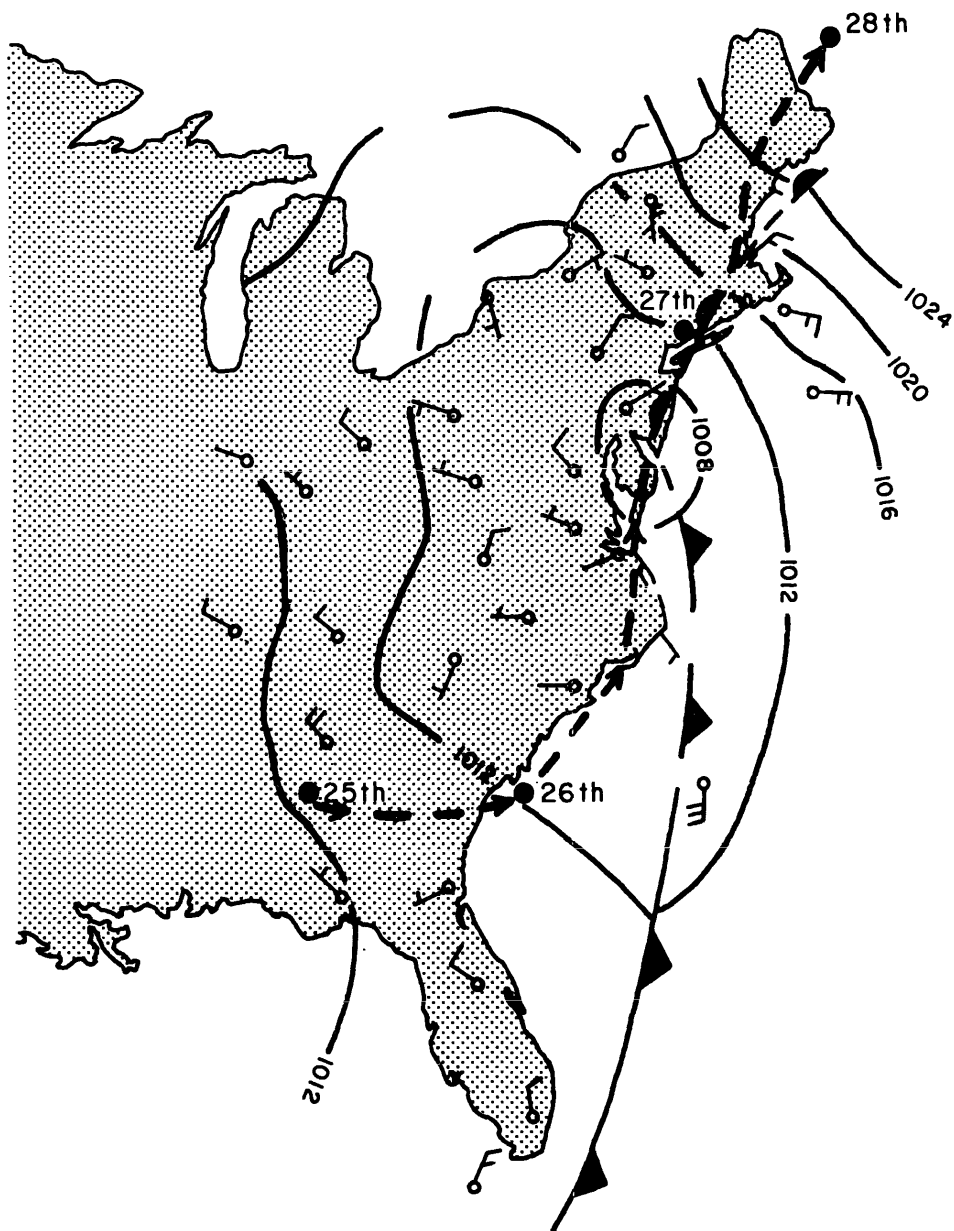
Current observations at R0 and R35 were made with four Braincon Type 1381 Histogram current meters moored on taut wires. At R0 the meters were set at depths of 1.6 m and at 10.8 m below the surface; at R35 they were set at 2.0 and 7.4 m. The meters were equipped with a vane for indicating current direction and a Savonius rotor for indicating speed. The meters recorded on film the direction, tilt and total number of revolutions over a twenty-minute period. The photographic film was developed and analyzed using a scanner interfaced with a tape recorder. Speed and direction were calculated from the digitized data. The longitudinal component of velocity was calculated for each 20-minute interval. Additionally, the mean non-vector average was calculated as also, the net non-tidal average for each tidal cycle. The records at R0 began March 21 and terminated April 19; at R35 they began March 23 and terminated April 13-14.

4. RESULTS

Storm and Runoff

The storm reached the U.S. Gulf Coast March 24-25 and traveled northward along the U.S. East Coast reaching the Chesapeake region March 27 (Fig. 4). It generated strong northeast winds in the region, but as it passed farther north winds shifted to northwest and diminished. Rainfall began on the Rappahannock watershed mid-day March 25 and continued for about 38 hours to 0400 March 27. Precipitation on the Piedmont watershed totaled 3.0 to 4.5 cm for the entire event, while on the coastal plain it totaled from 5.0 to 9.5 cm. Since rainfall was more or less simultaneous over the entire basin, runoff discharged into the estuary first from the lower tributaries and later from the mainstream drainage. The high water crest passed downstream from Remington to Fredericksburg, a distance of 48 km (30 miles) in 8.2 hours. The runoff produced water levels at Fredericksburg reaching a peak at 0630 on March 27, of 2.1 meters (7 feet) equivalent to a discharge of 358 m³ per second (12,800 cfs). As shown in Figure 5A, discharge rates display a simple hydrograph with a sharp peak on March 27 followed by a smooth recession March 28-April 18. A runoff event of this size is seven times the annual average discharge (Fig. 5A) and has a recurrence interval slightly greater than one year (Fig. 6). The March 27 discharge was one of five high runoff events during 1977-78. Although not a major flood, HIFLO discharge was one that occurs frequently, once a year on the average.

Sediment influx reached 4,800 tons per day at Remington, or about 10 times the daily average. For loads transported at Remington, the load per unit discharge was about average. Table 2 compares the sediment load and peak discharges of HIFLO with other big events in the Rappahannock basin. Farther downstream at Fredericksburg peak influx to the estuary head reached 12,300 tons per day or 21,000 tons per event over four days of the event, March 26-29.

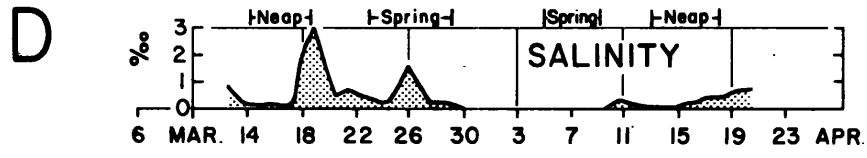
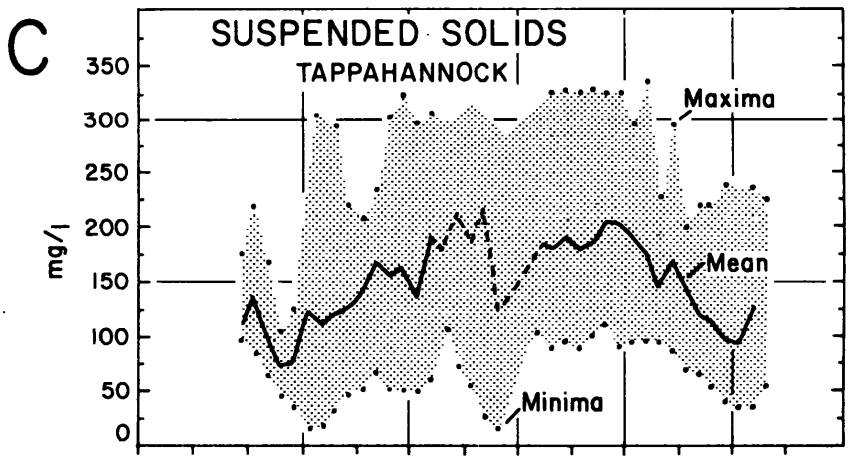
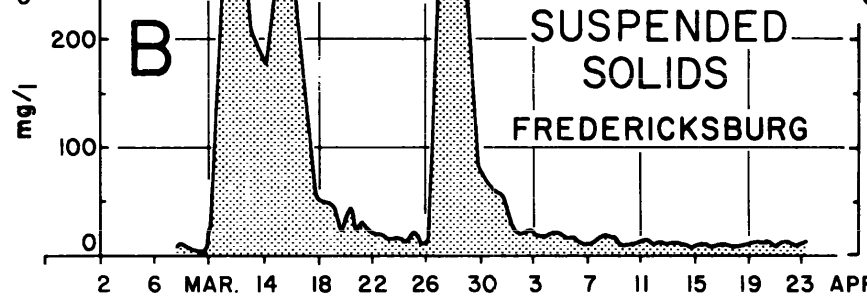
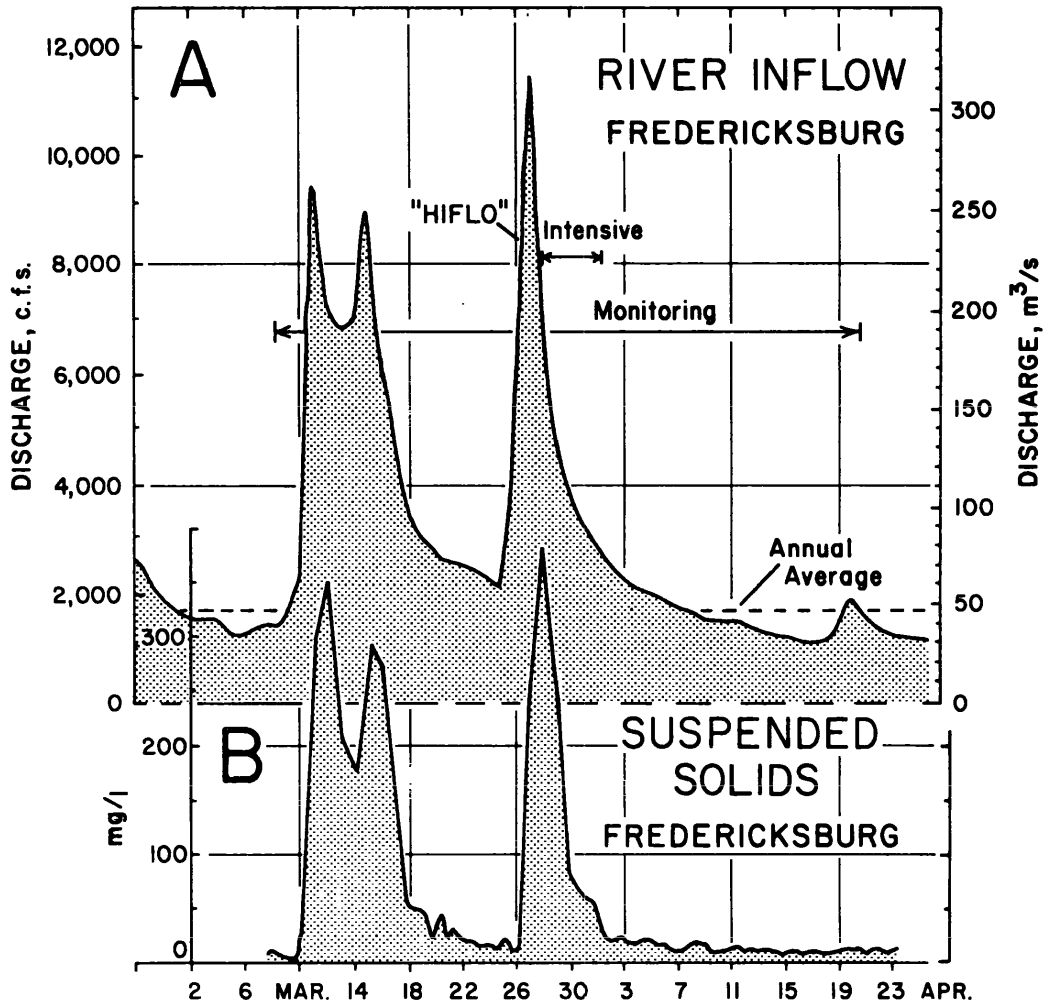


STORM TRACK

Figure 4. Track of the Storm of March 27 along the U.S. East Coast. Wind, fronts and pressure patterns at 0700 March 27, 1978; data from NOAA, National Weather Service.

Figure 5. Time variations of hydrologic and sedimentologic features:

- A. Hydrograph of daily average river inflow at Fredericksburg, March 8-April 21, 1978; survey periods for intensive longitudinal slack water observations and monitoring, arrows.
- B. Corresponding time distribution of daily average suspended sediment (solids) load at Fredericksburg.
- C. Time-distribution of mean daily suspended sediment load near the bottom at Tappahannock; extrapolated data, dashed; daily maximum and minimum values, dots.
- D. Time-distribution of daily average salinity near the bottom at Tappahannock. Neap and spring indicate actual range of the tide.



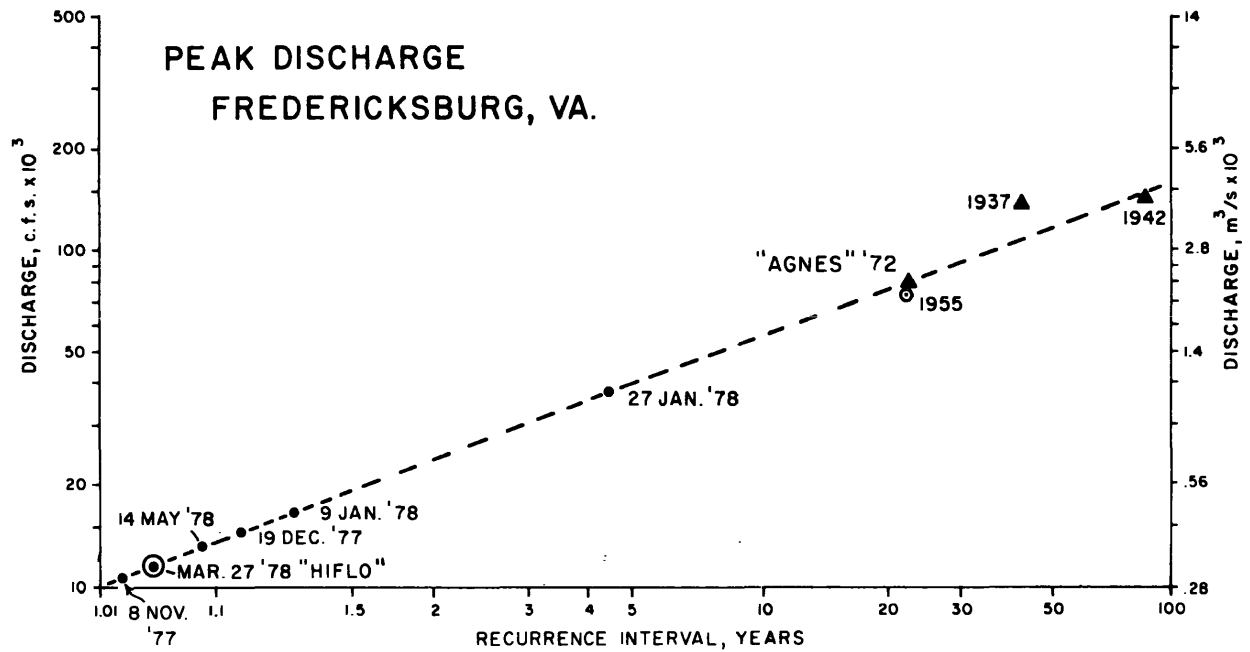


Figure 6. Recurrence interval for peak discharge at Fredericksburg, based on Virginia Division of Water Resources (1970).

Table 2. Comparison of HIFLO sediment loads and peak discharges with other events recorded by U.S.G.S. at Remington since 1951.

Date	Storm Sediment Load, tons	Storm Period, Arbitrary, days	Peak Discharge m/s
Aug. 19, 1955	43,900	7	1263
Mar. 20, 1963	82,100	10	195
June 22, 1972 (Agnes)	41,500	11	1296
Mar. 20, 1975	71,300	9	501
Sept. 26, 1975	107,300	6	397
Jan. 27, 1978	50,710	4	109
Mar. 27, 1981 (HIFLO)	8,146	4	358

Tide Effects

During passage of the storm that generated HIFLO, March 25-28, the tidal height, which was recorded on an NOS gage near the estuary mouth (New Mill Creek), reached 42 cm above predicted heights. The increased tidal heights, more than 30 cm above predicted heights, began about midnight March 24 or 54.5 hours before the peak river inflow at Fredericksburg. Tidal heights of both high and low water, returned to near-normal predicted heights by midnight March 28. Timing of the tidal height departures suggests that the increased water levels at the estuary mouth occurred in response to meteorological forcing as wind stress and atmospheric low pressure rather than river discharge. Despite high river inflow, the tide continued to rise and fall throughout the estuary.

Salinity Response

High river inflow lowered salinity and increased haline stratification in the estuary. At Tappahannock water freshened quickly, within 24 hours after rainfall began. Continuous recordings showed salinity decreased from 1.5⁰/oo at 0200 March 26, to nearly zero at 1100 March 27 (Fig. 5D). Since the initial change occurred mainly before the mainstream crest passed Fredericksburg, initial freshening was first produced by inflow from tributaries downstream of Fredericksburg. By March 28, one day after high inflow at Fredericksburg, the inner limit of salty water, i.e. 0.5 ppt in surface water, shifted to its most seaward position, 12.8 km (8 miles) downstream of its position prior to high inflow (R36). Near-bottom salinity also dropped to nearly zero on March 28 in the same reach (R28-R36), while at the estuary mouth salinity dropped by about 2 ppt. By March 30, stratification intensified in the zone R20-R28. The maximal vertical gradient reached 0.9 ppt per meter depth at R25 (Fig. 7A). However, our longitudinal sections during the high inflow period March 28-April 10 (Fig. 8) reveal the estuary-wide salinity distribution varied within narrow limits. Although salinity was markedly depressed at the head of the salt intrusion, the horizontal salinity gradient in the lower estuary was maintained (Fig. 7B). The indirect effect of high river discharge was to freshen water throughout the entire estuary by 2 to 4⁰/oo and to maintain this lowered level for about 20 days. Near-

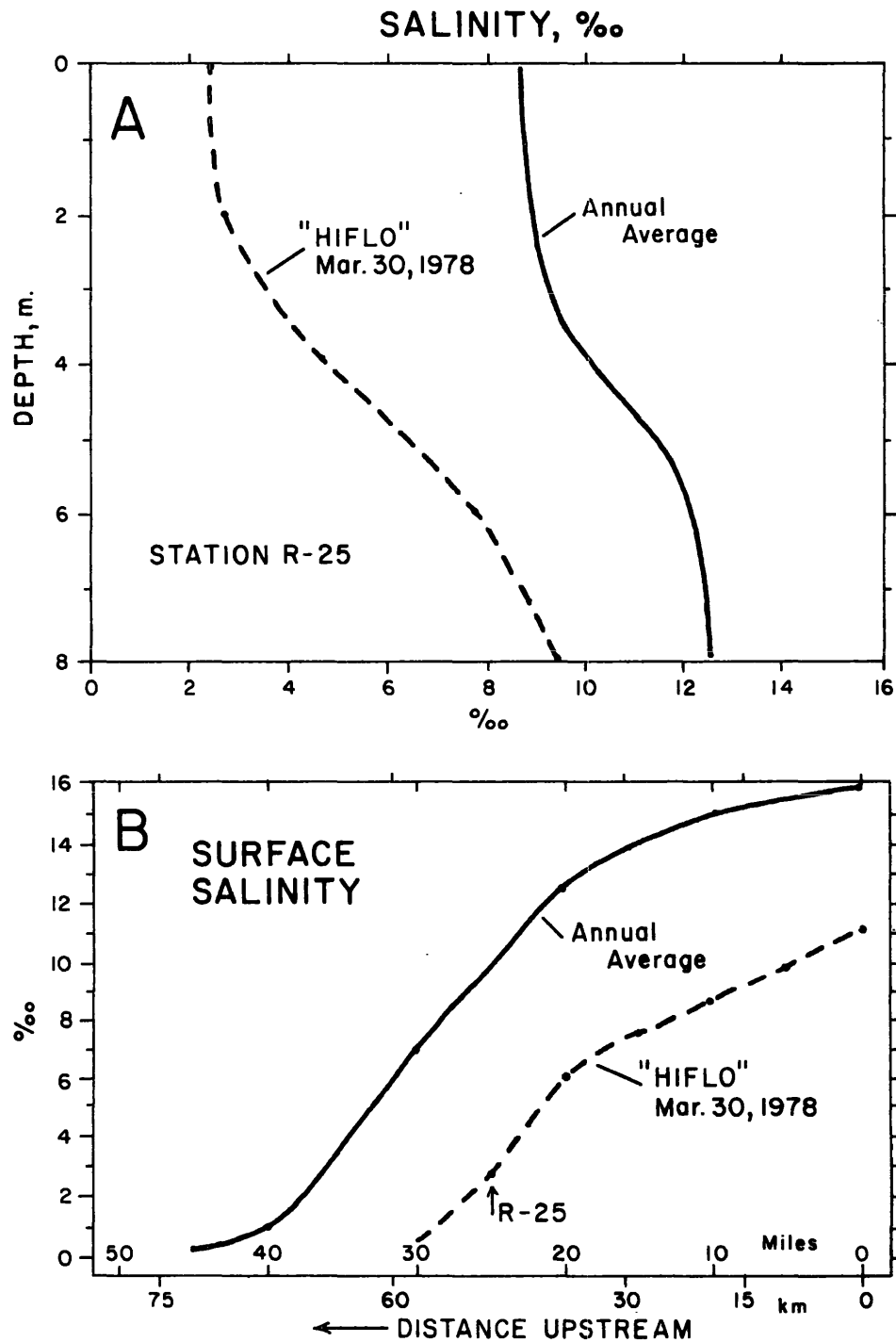


Figure 7A. Vertical distribution of salinity at R25, March 30, a time of maximum stratification, in relation to 21-year average at the same station.

B. Longitudinal distribution of surface salinity, March 30, in relation to 21-year average.

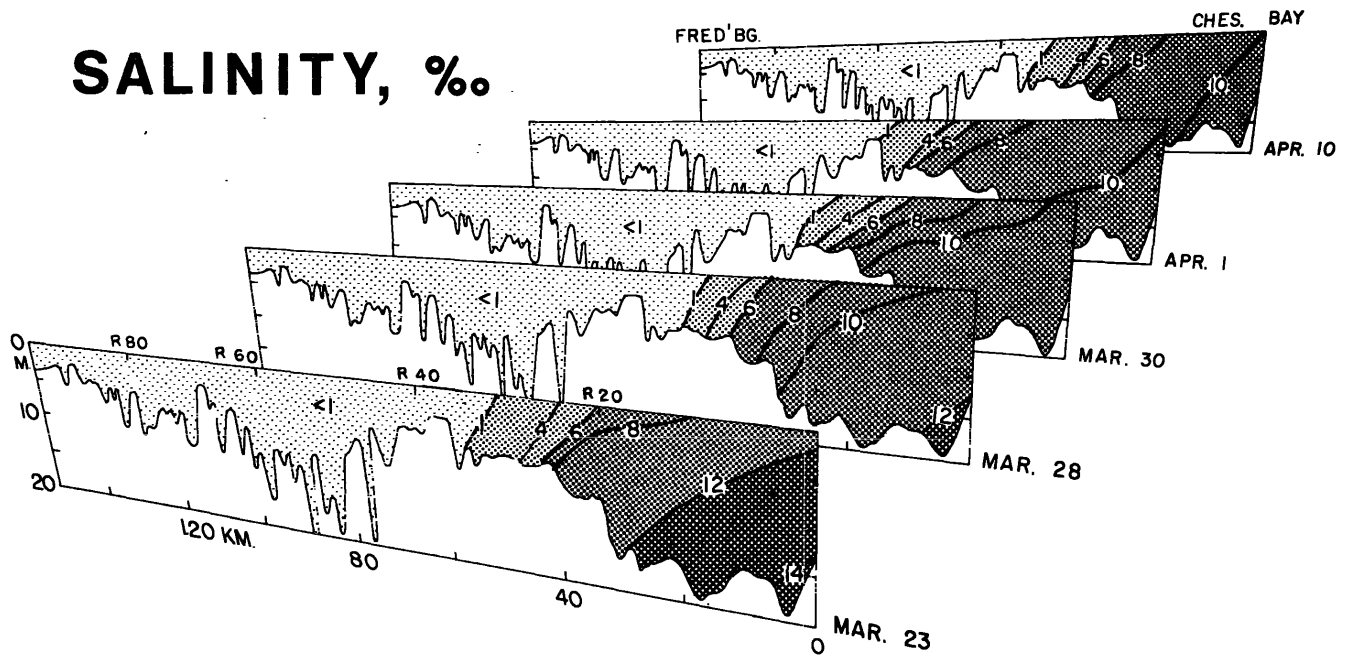


Figure 8. Longitudinal distribution of salinity at slack water in selected perspective sections from the estuary mouth to Fredericksburg, March 23-April 10, 1978.

bottom salinity at Tappahannock began to recover significantly, April 15 (Fig. 5D). In brief, the salinity response consists of: (1) a seaward shift in the inner limit of salty water, (2) increased stratification and (3) a slight freshening throughout the estuary. The estuary retained its salt intrusion as well as its partially-mixed regime through all stages of high inflow.

Flow Response

Current velocity observations at R0 and R35 display three modes of response: (1) a tidal variation at a time scale of hours, (2) a net non-tidal variation over one tidal cycle of about $12\frac{1}{2}$ hours, and (3) the net non-tidal variations over 2 or more tidal cycles (days).

Before high inflow, March 24-25, current velocity recorded at Tappahannock (R35) displays a time-velocity curve with a maximum flood current of 69 cm per second and a maximum ebb current of 58 cm per

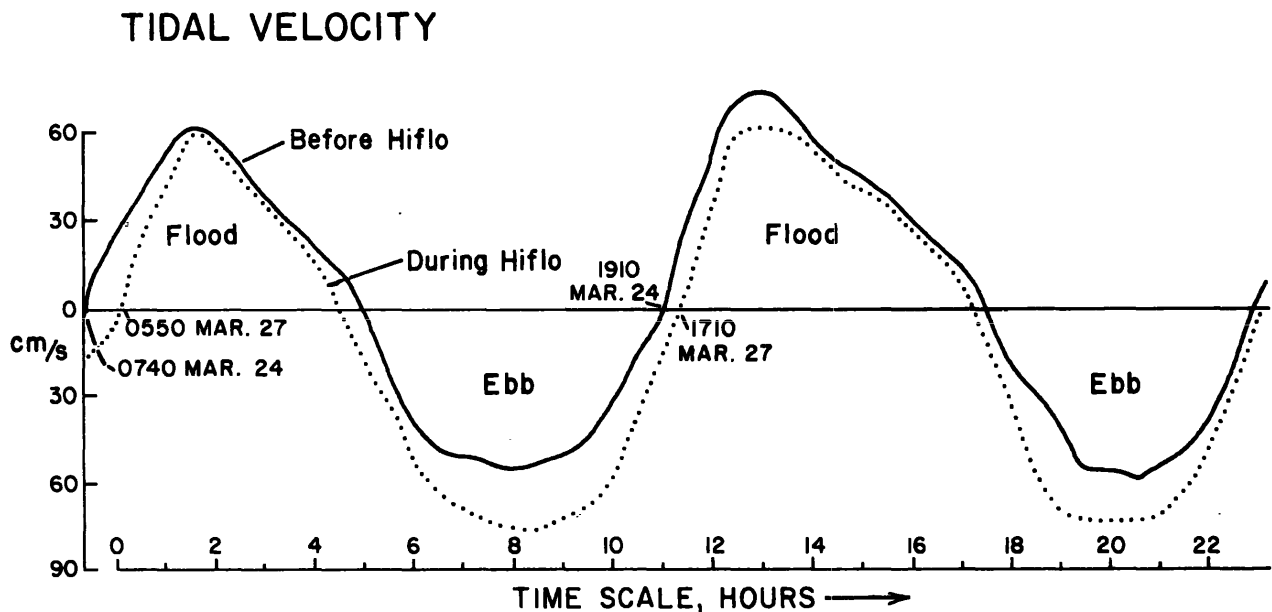
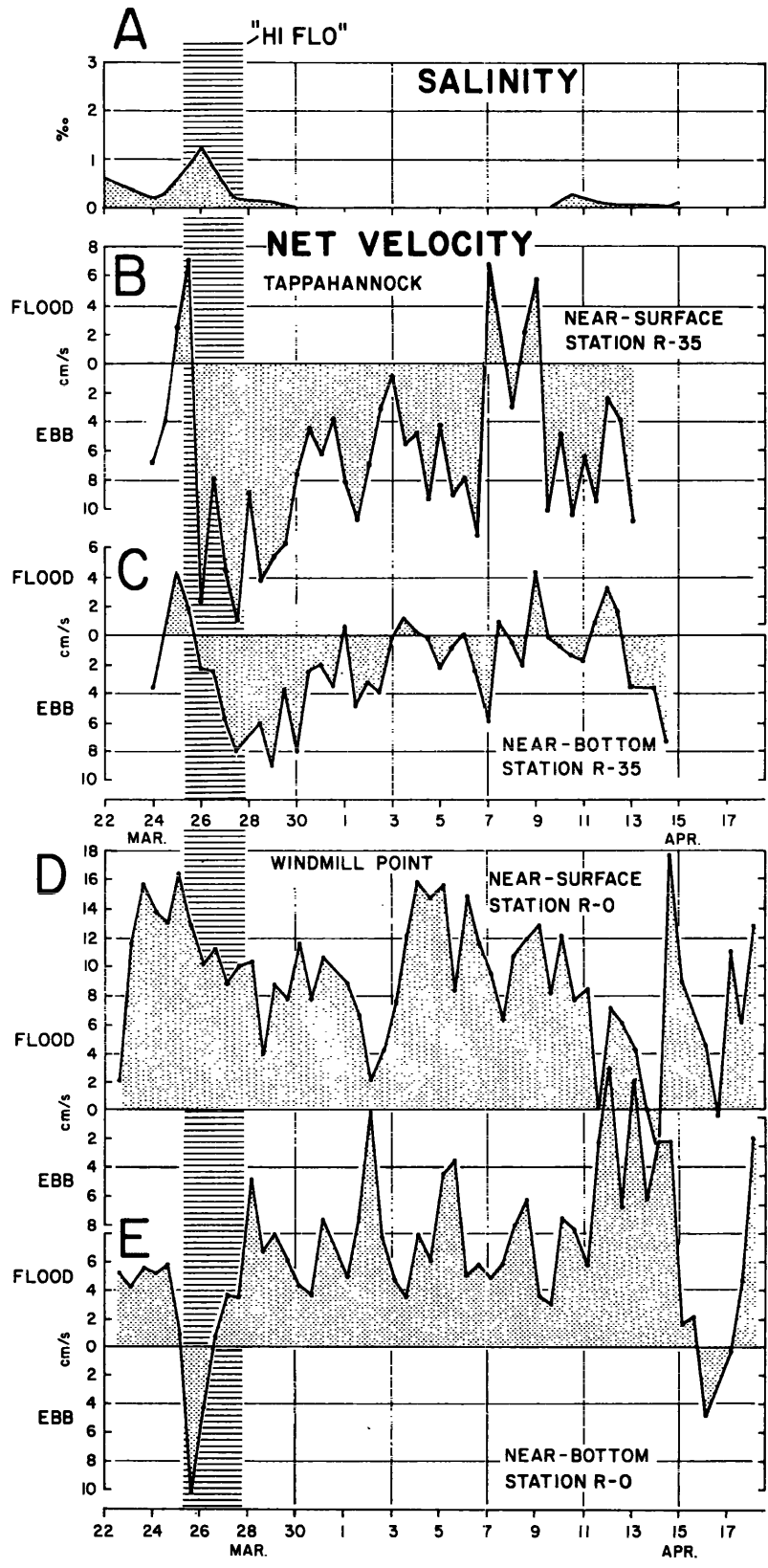


Figure 9. Time-velocity curves at R35 showing the change in magnitude and duration of near-surface flow, before and during high inflow.

second, Figure 9. During high inflow, March 27-28, the flood duration was shorter by about 12 percent than before high inflow, and the flood amplitude was reduced by about 10 percent. By contrast, the ebb duration increased by about 14 percent compared to the ebb duration before HIFLO. Moreover, the ebb magnitude was about 20 percent greater than before high inflow. These changes are likely produced by the high river discharge of HIFLO augmented by the release of "excess" water forced into the estuary by wind and pressure during early stages of the storm. Despite these forces, tidal currents continued to ebb and flood throughout the estuary. Because of their large amplitude, tidal currents are responsible for mixing fresh and salt water and they create turbulence that is responsible for resuspending much sediment from the bed.

At Tappahannock, R35, before high inflow, March 23-25, the near-surface mean non-tidal velocity over four tidal cycles was 1.6 cm per second seaward, while the return near-bottom mean non-tidal velocity was 4.6 cm per second landward (Fig. 10B, 10C). These trends reveal a two-layered estuarine circulation that is confirmed by the salinity structure of March 23 (Fig. 8).

- Figure 10.
- A. Time-distribution of daily average salinity near the bottom at Tappahannock in relation to HIFLO.
 - B. Time variations of net non-tidal velocity, one tidal cycle at a time, for near-surface (2 m depth) at R35, Tappahannock.
 - C. Corresponding net velocity for near-bottom (7.4 m depth).
 - D. Time variations of net velocity at R0, Windmill Point for near-surface (1.6 m depth).
 - E. Net velocity for near-bottom (10.8 m) depth from March 22 to April 18, 1978, at R0.



At the onset of HIFLO, March 25-26, net velocity at R35 quickly changed direction and ebb flow accelerated (Fig. 10B, 10C). Near-surface ebb reached 16.5 cm per second or about 10 times the speed before high inflow (Fig. 10B). The strong seaward flow continued for four days, to March 30, in both near-surface and near-bottom water (Fig. 10B, 10C). Consequently, high inflow, augmented by meteorological forces, changed the pattern of circulation in the zone R30 to R38 from a two-layered estuarine circulation to a seaward river circulation at all depths. The change is confirmed by the rapid drop of near-bottom salinity at Tappahannock, March 26 (Fig. 10A).

After high inflow, March 30, net velocity in both near-surface and near-bottom water at R35, diminished to 0.9 to 10.7 cm per second, mainly seaward (Fig. 10B, 10C). However, progressive recovery was interrupted April 7-10 by a landward flow in near-surface and near-bottom water. This trend was associated with passage of another storm system. Since river inflow was low during this period, the velocity fluctuations must have been generated solely by pressure and wind forces. Winds mainly blew from the northeast, April 6-8 and then April 8-9 from the northwest. Between April 9 and 15, net velocity resumed a two-layered flow with a mean near-surface speed of 6.2 cm per second seaward and a near-bottom speed of 3.7 cm per second landward (Fig. 10B, 10C).

At the estuary mouth, R0, off Windmill Point, before high inflow March 23-25, the mean non-tidal velocity over four tidal cycles was 14.4 cm per second landward in near-surface water and 5.2 cm per second landward in near-bottom water (Fig. 10D, 10E). This trend is part of a two-way estuarine circulation whereby net flow is directed landward through the mouth on the north side and seaward from the estuary on the south side.

At the onset of HIFLO, March 25-26, the near-surface landward flow diminished by about 30 percent while the near-bottom flow changed markedly (Fig. 10D, 10E). It changed direction from landward (flood) to seaward (ebb) for two tidal cycles and reached a peak net velocity of 10.3 cm per second. Thus, HIFLO temporarily reversed the estuarine circulation in the mouth. After HIFLO, March 28, the near-bottom flow resumed its landward

direction with speeds ranging 4 to 12 cm per second whereas the near-surface flow continued to drop irregularly. This trend is comparable to the decreasing seaward flow at R35 during the same period. While decreasing river inflow may be responsible for the trend at R35, a lag in the same inflow may be responsible for the trend at R0.

A return of normal flow at R0 was interrupted April 11-14 by a meteorological disturbance that strengthened the near-bottom landward flow and slowed the near-surface landward flow. This disturbance consisted of winds blowing from the west, directed seaward and southeast. The trend contrasts with the opposite current response of northeasterly winds associated with HIFLO. Therefore, velocity variations at the mouth are mainly induced by meteorological forces rather than high river inflow.

Although the current observations exhibit variations associated with meteorological conditions, the net non-tidal velocity, averaged over 21 to 28 days (Table 3), shows the flow is consistent with the estuarine circulation of a partially mixed estuary. This is partly confirmed by the salinity structure, Figures 7A and 8. At R35 in nearly freshwater the net velocity is seaward at both depths. At R0 on the north side of the mouth, net velocity is landward at all depths. Although the surface current has an anomalous landward direction, this is not unexpected since prior current observations of VIMS display a seaward net velocity at all depths on the south side of the mouth.

Table 3. Net Non-Tidal Velocity at Station R0 and R35 Averaged Over 21 and 28 Days Respectively. Seaward is Minus; Landward is Positive.

Station R35 (VIMS)			Station R0 (CBI)		
<u>Depth,</u> <u>m</u>	<u>Speed,</u> <u>cm/s</u>	<u>Direction,</u> <u>degrees</u>	<u>Depth,</u> <u>m</u>	<u>Speed,</u> <u>cm/s</u>	<u>Direction,</u> <u>degrees</u>
1.9	-1.2	75	3.1	+9.6	281
7.4	-1.8	72	10.9	+7.2	273

Suspended Sediment Response

Sediment influx from the river at Fredericksburg generally followed the daily water discharge (Figs. 5A, B). However, our continuous suspended solids records reveal that the peak sediment load lagged behind the peak discharge by 11 hours. Consequently, the bulk of the sediment load was introduced as the inflow receded.

In the upper and middle estuary our longitudinal slack water sections of March 28 display relatively high loads, greater than 100 mg/l, in the form of patches or fragmented aureoles centered on R35 and R80 (56, 128 km) above the mouth, Figure 11. The upper aureole, which has an asymmetrical distribution with higher concentrations on its seaward side, represents the recent influx supplied by HIFLO. The lower aureole consists of a turbidity maximum that

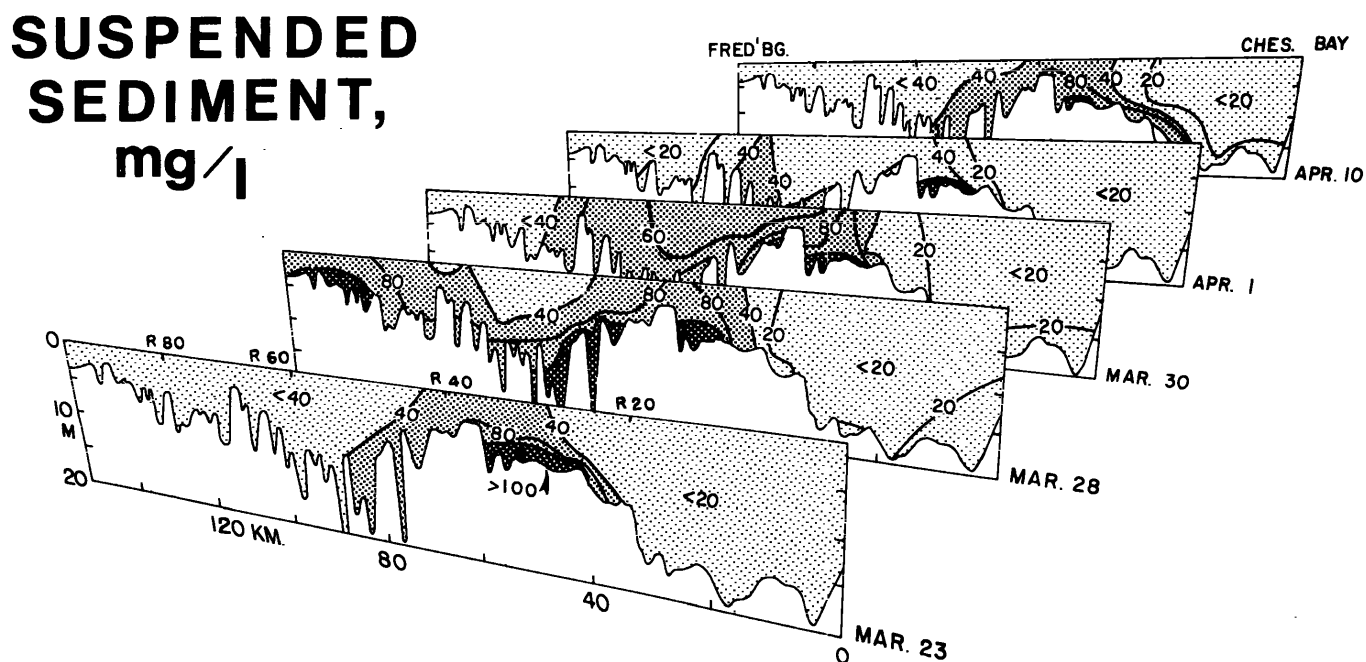


Figure 11. Longitudinal distribution of suspended sediment at slack water in selected perspective sections from the estuary mouth to Fredericksburg between March 23 and April 10, 1978.

existed before high river inflow began, March 23. The maximum has been observed to reside just landward of the inner limit of salty water (Nichols and Thompson, 1973). By March 30 concentrations in both aureoles diminished by more than 20 percent. Whereas the upper aureole moved seaward about 46 km (25 miles), the lower aureole maintained the same position (Fig. 11). By April 1 concentrations of both aureoles diminished to less than 55 mg/l. On April 10, only the lower aureole remained intact. The bulk of the sediment influx was "lost" in the upper estuary during the first four days of high inflow. Development of the lower aureole, or turbidity maximum, is associated with the current null zone and sediment resuspension from the bed.

Our continuous measurements of suspended sediment near the bed at Tappahannock, display marked variations at different time scales. There are generally two pronounced maxima and minima each day, ranging over 200 mg/l, that represent periodic resuspension. Maxima occur near maximum tidal current, either ebb or flood, whereas minima occur near slack water. Superimposed on these variations there is a fortnightly trend for daily mean and minima concentrations to increase as the tide range proceeds from neap to spring (Fig. 5C). By contrast, concentrations decrease from spring to neap range (Fig. 5C). Of note, the concentration peaks and troughs lag the tidal periods by 2 to 4 days. Because HIFLO occurred during spring tide range, sediment variations produced by the tide and the neap-spring cycle are much greater than the variations produced by river inflow. The lack of any significant increases in the daily mean concentrations after high inflow suggests that the direct impact of river-borne sediment influx on middle and lower reaches was limited.

The net flux of suspended sediment was investigated by using longitudinal distributions of sediment and salinity as input to a box model following the formulations of Pritchard (1969) and Officer (1980). Results reveal that net fluxes from the river and the Bay are of about the same magnitude totaling about 2035 tons per day each (Officer and Nichols, 1980). Deposition is predicted in a zone seaward of the turbidity maximum between stations R25 and R5. The model confirms that the turbidity maximum is a phenomena related to the estuarine circulation.

Dispersal of sediment during HIFLO followed several routes. The mainstream influx from the Piedmont moved downstream through the upper estuary and deposited mainly in freshwater reaches (R55-R65) during late stages of high river inflow. A small fraction which remained in suspension, moved farther seaward into the zone of the turbidity maximum. This load, together with the lateral influx and material resuspended from the bed of lower reaches, accumulated in the current null zone and intensified the turbidity maximum. Since transport of suspended sediment follows the net non-tidal flow (Nichols, 1977), it seems likely that sediment remaining in suspension for a long time is transported in the estuarine circulation. The basic pattern is: seaward through the upper layer, downward by settling into the lower layer and landward through the lower layer (Fig. 12). HIFLO temporarily changed the pattern in channel reaches that were freshened, i.e. between R36 and R28 (Fig. 12). As shown by our near-bottom current measurements, net velocity changed from net landward to net seaward flow March 25 (Fig. 12), presumably as the current null zone moved downstream.

DISPERSAL PATTERNS

Middle and Lower Estuary →

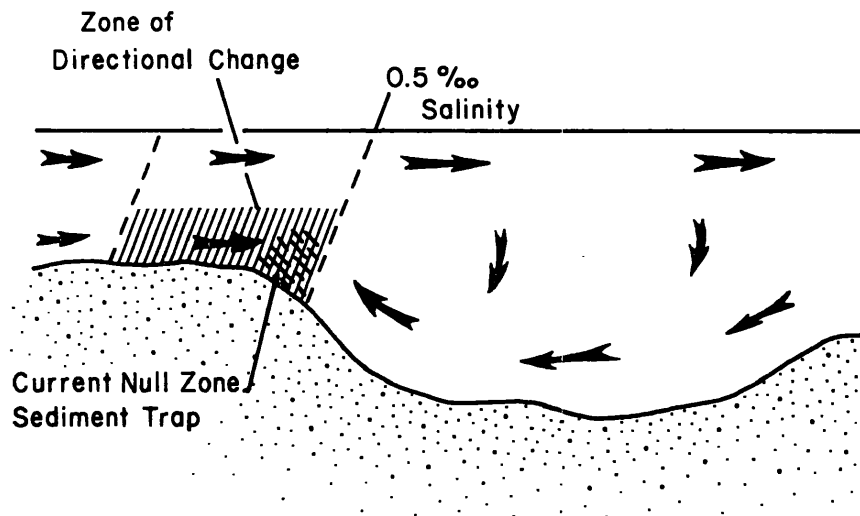


Figure 12. Schematic diagram of sediment dispersal pattern showing a zone of directional change produced by high inflow.

A change in the transport direction in the zone of the turbidity maximum can mix and redistribute sediment derived from river and seaward sources. Response time at the salt intrusion head is rapid because the dynamic balance between fresh and salty water is very sensitive to changes of inflow. Mixing is fast, dilution is high, and near-bottom flow is subject to reversal. Instead of flushing sediment loads through the estuary, high river inflow enhanced the effectiveness of the hydrodynamic regime to trap sediment. Entrapment is favored by increased stratification, accelerated landward flow through the lower estuarine layer and strengthening of the near-bottom convergence between seaward river flow and landward estuarine flow.

Response Sequence

The events triggered by HIFLO followed a sequence in response to meteorological forces and high river inflow. This sequence predicts what can happen in the Rappahannock during future events like HIFLO; it indicates the stages that may occur in other partially-mixed estuaries at similar time scales. The sequence and associated characteristics consists of:

1. Initial Response. Onset of storm, and high rainfall, 1 to 1½ days. Rising storm tide, surface wind drift landward and net current reversal in bottom water near mouth.
2. Shock. One to two days; continued rainfall, flooding of lower tributaries. Abrupt salinity drop at salt intrusion head; strong surface net flow seaward and near-bottom current reversal at head; increased net landward flow near-bottom at mouth; increased haline stratification.

Peak mainstream flooding on fall-line followed by peak sediment influx and lowering of storm tide, maximal seaward surface flow near head of salt intrusion, maximum salinity depression, resident turbidity maximum intensified.

3. Rebound. One to two days; receding river inflow and sediment influx. Normal tide level, diminished net seaward flow at salt intrusion head and diminished net landward flow at mouth; maximum salinity stratification; river-borne sediment load shifts seaward into upper estuary and diminishes; resident turbidity maximum decays.

4. Recovery. Eight to twelve days; subsiding river inflow and occasional meteorological disturbances. Net flow regains normal speed, salinity remains low but increases at head, turbidity maximum persists with low suspended loads.

Table 4 compares the magnitude of different response variables under normal and peak HIFLO conditions.

Table 4. Comparison of Response Variables Under Normal and Maximal HIFLO Conditions.

<u>Variable</u>	<u>Normal</u>		<u>HIFLO*</u>	
	Estuary Head**	Estuary Mouth**	Estuary Head**	Estuary Mouth**
Salinity, ‰ surface	3.8	16.2	0.1	10.0
Net Current Velocity, cm/s, surface	-5.4	-4.0	-17.8	+9.0
Tide Range, cm	51	33	-	60
Peak Tide Height, cm	59	40	-	42
Total Suspended Sediment load, mg/l				
surface	22	3.2	85	10
bottom	35	4.5	161	38

*Maximum values.

**Estuary head located in vicinity of R35, Tappahannock; mouth at R0, Windmill Point.

-Seaward direction.

-Landward direction.

Particle Size

Most suspended sediment introduced into the upper estuary during high inflow consisted of fine silt and clay. During high sediment influx March 28, particle size of near-bottom suspended material became smaller with distance seaward through freshwater reaches R65 to R35 (Fig. 13). Mean size diminished from 11.5μ to 5.8μ with finest sediment at R30, the zone of the turbidity maximum. When sediment loads diminished by April 1, the size distribution in freshwater reaches became finer and more uniform, whereas in saline reaches size coarsened seaward. When the natural samples were disaggregated by dispersion in Calgon and agitation, mean particle size of samples from saline reaches was reduced to the range 0.5 to 4.6μ with greatest reduction near the mouth (Fig. 13). The size reduction gives an indication of the relative degree of aggregation or agglomeration of the natural material.

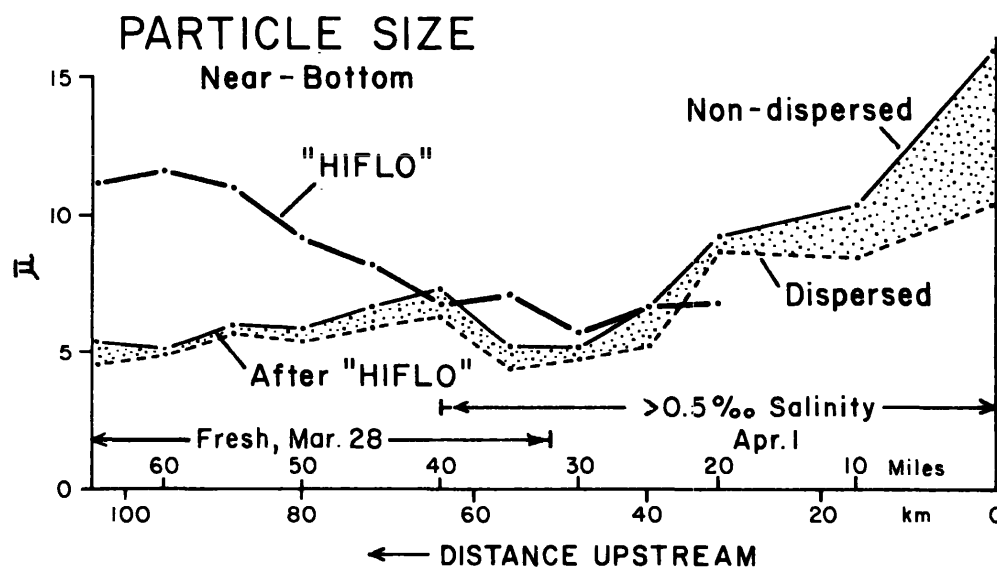


Figure 13. Seaward change of mean particle size in near-bottom suspended material collected during high sediment influx March 28 and after high inflow April 1. Dotted pattern represents zone of size reduction after sample dispersion. From analysis of total sample except for non-dispersed samples of April 1 which were estimated total sample from size distributions coarser than 2.8μ .

Analyses of SEM micrographs of samples taken on April 1 show that samples from brackish water (R25 and R30) contain substantial percentages of aggregates, which have individual mineral grains, biogenic fragments, and living biota incorporated in an organic matrix. The mean diameter of these aggregates is considerably larger than the diameters of individual grains with which they are associated in the sample (Appendix 1). The individual grains included within the aggregates are close to the same size, or slightly smaller, than the unassociated single grains in the sample. Individual grains are relatively more common than aggregates in fresh water.

Because of the small sample size, noise in the data causes problems in establishing trends from fresh to brackish water. Examination of the modal diameter of the count statistics suggests a seaward increase in overall particle size from 1.6 μm on the surface at R60 to 4.6 μm in samples from the surface and 0.3 m off the bottom at R30 (Appendix 2). Samples from near the bottom have a much higher probability of including resuspended material during intensification of the river-estuarine current convergence. Histograms of the size distribution graphically illustrate seaward changes for count statistics (Fig. 14).

The seaward increase in modal diameters appears to substantiate the data obtained from the Coulter Counter on the same set of samples (Fig. 13). Intuitively, we would expect the particle size to diminish with distance seaward. The increase in size, coupled with a reduction after sample dispersion, indicates an active aggregation process.

Particle Composition

We discriminated between seven types of particles in the SEM micrographs. Clean grains had surface microtextures and laminae readily visible with good relief. Coated grains had indistinct microtexture and blurred laminae, cleavage faces, and fracture surfaces. We assumed that the coatings were organic material (Pierce and Siegel, 1979; Eisma, et al., 1980). Biogenic particles were living microbiota or fragments of tests. Clean aggregates were groupings of individual grains into multi-component particles without

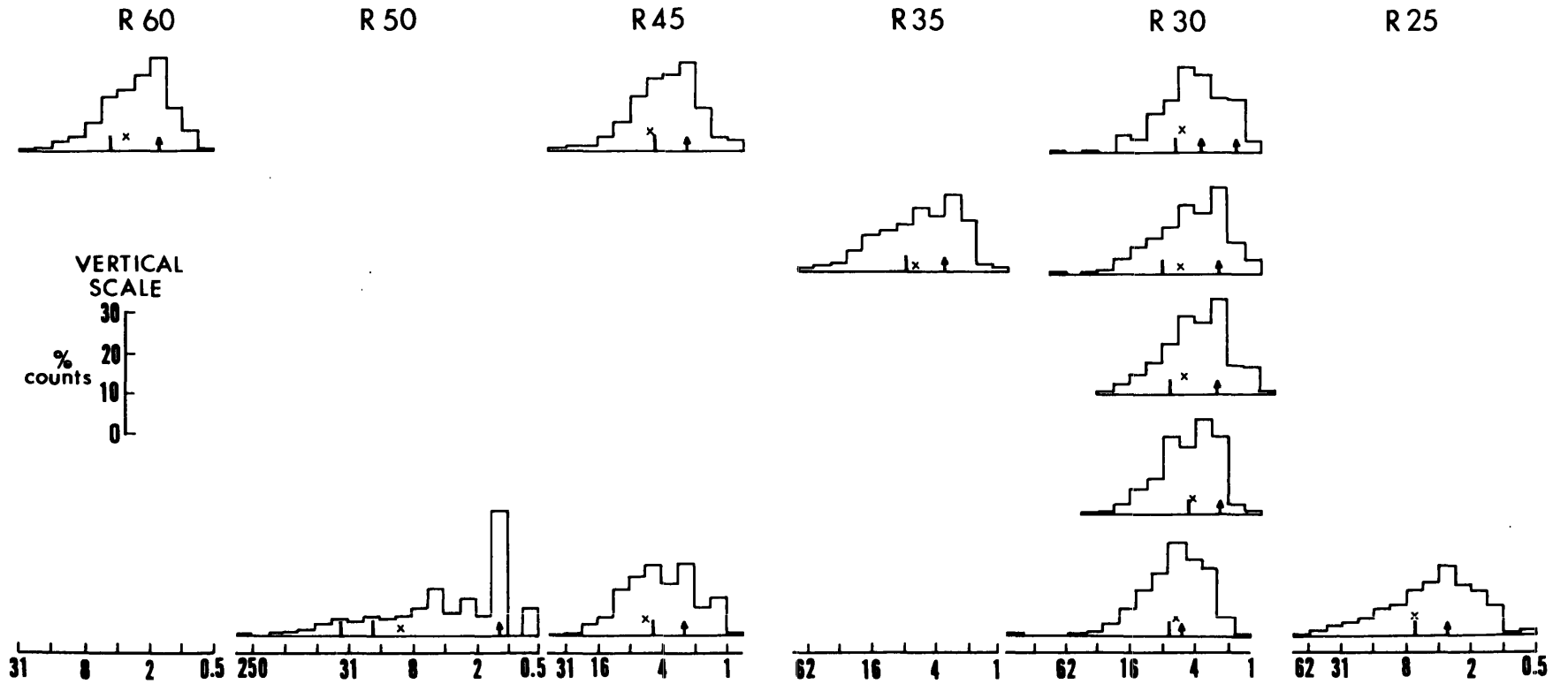


Figure 14. Histograms of count statistics for samples analyzed by SEM. Scale below each histogram indicates size in micrometers. Vertical scale is % counts. Arrow denotes grain mode; bar, aggregate mode; X, arithmetic mean diameter. From samples of April 1, 1978.

any visible matrix. Aggregates with an organic matrix were groupings of coated mineral grains and biogenic particles in a matrix, which has no apparent ordered structure. We assumed the matrix to be organic material. Organic material is a mass of apparently soft material with no ordered structure and no included biogenic particles or mineral grains. This material is generally flattened on the filter although it gives the appearance of having been spherical. Fecal pellets are cylindrical masses of material with the long axis several times the length of the short axis. Particles having the appearance of fecal pellets are rare. Some particles classified as aggregates with an organic matrix may be fecal pellets in the process of being broken up. Not all types of particles were discriminated in all samples; some were absent. Others occurred in such low numbers as to be relatively insignificant in the counts.

The sample of surface water from R60, April 1, primarily has single grains or relatively simple associations of grains (Appendix 3). Relatively few of the grains have coatings that obscure the surface texture. All of the material is small, 62 percent having a projected diameter of less than $2.8\mu\text{m}$. The overall appearance gives the impression of an incompletely disaggregated soil. Average diameter of the total sample is $3.4\mu\text{m}$ (Appendix 1).

Many very small grains and large loose aggregates of grains were present 0.3 m above the bottom at R50 (Fig. 14). Some of the aggregates looked like "rafts" of particles with a minimum of matrix (Appendix 4A). Other aggregates appeared as branched strings, easily disaggregated (Appendix 4B). Much of the filter surface was heavily coated with aggregates and grains. It was difficult to obtain a magnification that permitted a view of an entire large aggregate (200X) as well as permitting one to distinguish the small grains, best shown at magnifications of 2000X. The largest particle encountered was at this station (R50), an aggregate with a projected diameter of $339\mu\text{m}$. The aggregates appear to be loosely bound and could be broken up easily. Most of the single grains are clean, 46 percent of the total particles counted. If some of the loose aggregates were broken up, the number of grains would be greater. Although a greater number of aggregates are classified as having an organic matrix, the amount of matrix

is limited. This sample had the largest particles, the smallest individual grains and the largest average diameter. It is entirely possible that some resuspension of bottom material has occurred, although it is difficult to understand how the friable-appearing aggregate could withstand resuspension. The large number of very small individual particles would suggest disaggregation.

Individual grains constitute 47 percent of the total particles in the surface water at R45, most having a coating. Aggregates, slightly more than half of the particles, are held together mostly with organic material (Appendix 4C) although the amount of organic matter is limited. Some free organic matter is present, although it accounts for less than 3 percent of the total number of particles. The average diameter of the total sample is $4.5\mu\text{m}$ (Appendix 1).

The near-bottom sample at R45 had about the same proportion of aggregates as the surface sample (Appendix 3). More individual grains were clean than coated, as opposed to those in the surface. The average diameter was $5.8\mu\text{m}$.

Only one sample was analyzed for R35. A large part of the filter surface is heavily coated with material, making it difficult to decide whether some of the aggregates might have formed during the filtration. Aggregates outnumber single grains. Most aggregates have what appears to be an organic matrix, more complex than those from upstream, and they have a larger projected diameter (Appendix 1; Appendix 4D). There is more biogenic debris and whole organisms than at the previous stations. Although clean and coated grains were not discriminated in the counts, very few grains have clear fracture and cleavage surfaces, suggesting the presence of a coating.

Samples were taken from 5 depths at R30. The average projected diameter of $5.6\mu\text{m}$ is the largest of samples from surface waters, except that at R50 (Appendix 1). The average size of single grains at this station also is larger than those from samples farther upstream. This suggests that the suspensates at R30 (on April 1) were trapped in the river-estuarine convergence intensified by high river inflow. Presumably, the coarser particles

had been introduced into the zone during HIFLO. Similar sized particles in the freshwater reaches had settled out of suspension by the time of sampling. Alternately, some of the suspensates at R30 could be resuspended sediments deposited at this location during or shortly after HIFLO.

All grains in samples from this station (R30) were coated (Appendix 5A) except for about 6 percent of the total number found at a depth of 1 m above the bottom. All aggregates in the surface waters had an organic matrix (Appendix 5B). These complex aggregates, with an organic matrix, outnumber loosely-bound, clean aggregates at all depths (Appendix 3).

Some small particles, around $2\mu\text{m}$ in projected diameter, may be similar to those reported by Eisma, et al. (1980). Such particles, in the Rhine Estuary, presumably are produced in salinities of about $2^0/00$. We did not discriminate in the counts such particles, although reexamination of the SEM micrographs suggest that a few particles, approximately $2\mu\text{m}$ in projected diameter, may be similar to those reported by Eisma, et al. (1980). The logical samples to contain these particles are at R30, surface and 2 m (Appendix 5D). No other micrographs had similar particles although some small grains, not examined with high magnification, could be similar in shape.

Only one sample from R25 was analyzed. At 0.3 m above the bottom, this sample had mainly coated grains and complex aggregates with some free organic matter (Appendix 5C). Resuspension of bottom sediments is a possibility here because of proximity to bottom.

Although the count statistics indicate that small grains far outnumber aggregates, the greatest volume of the suspended particles is found in the aggregates. The much larger diameters associated with the aggregates and the fact that they tend, in most cases, to be more equidimensional give them an overwhelming proportion of particle volume. Crude estimates of volume, assuming certain regular solids, indicate that the median diameter of volume statistics is greater than $11\mu\text{m}$ in all samples. For five samples, the median diameters of the volume statistics were larger than $31\mu\text{m}$.

The analysis of the SEM micrographs, although far from definitive, suggest processes involved in aggregation of single grains into multicomponent particles. Single grains, eroded from the uplands, acquire a coating of organic material, either by direct absorption (Meyers and Quinn, 1973; Pearl, 1974) or by settling of microorganisms and uptake of macromolecules (Loder and Hood, 1972). Growth and increasing complexity of aggregates occurs by addition of more grains, more organic matter, and biota (Pierce and Siegel, 1979).

5. SUMMARY

The sediment response triggered by the HIFLO event consisted of both direct and indirect effects. The mainstream inflow produced high suspended sediment loads in the upper estuary that extended downstream 60 km from Fredericksburg. As inflow subsided and spring tidal currents waned, most of this load deposited in the upper estuary. Potential depositional zones include the shipping channel floor, quiet water lateral reentrants or embayments, and bordering marshes. These sites are regarded as temporary storage basins from which sediment can re-enter estuary water during the next larger flood and thus, resume downstream transport. The HIFLO observations suggest that transport through freshwater reaches takes place in stepwise processes involving temporary accumulation followed by resuspension and downstream transport.

The indirect response to high inflow consists of hydrodynamic changes affecting sediment transport at the inner limit of salty water. By enhancing stratification, displacing the inner limit of salty water and shifting the null zone seaward, conditions for sediment entrapment improved and the turbidity maximum intensified.

The HIFLO observations suggest that the turbidity maximum does not require a direct influx of river-borne sediment for its development. Instead, it can be intensified, and perhaps created, by sediment supplied from local sources at times when the river-estuarine current convergence is strengthened.

6. COMMENTARY

The HIFLO experiment successfully provided synoptic field observations of a moderate-sized event over a 144 km (90 mile) length of estuary. Besides providing a wealth of new observations, it demonstrated the capability of CRC institutions to carry out and coordinate field programs. This capability can be extended to other transient events like hurricanes or storm surge, red tides, accidental chemical or oil spills, explosions, derailments or ship collisions, crab-fish kills, acid dumps. HIFLO, however, was scheduled for a fixed site and it was more predictable than some other types of events. Other types of events may be more difficult to observe. Other areas may lack extensive baseline data, particularly for contaminants.

Lessons learned from HIFLO include: (1) extensive planning, coordination and logistic support are essential for the success of a multi-institutional field program responsive to such events; (2) instrument intercalibration and a procedural "shakedown" is highly desirable to insure comparability of measurements; (3) observations should be simple and standardized so that they can be made by different crews or observers; (4) logistics should include mobile field crews for rapid deployment wherever an event occurs; (5) to respond to a selected event, contingency plans for action, communications and availability of equipment are essential. It remains to determine: What events should be studied, either for scientific value, for resource management or for health and seafood resources? What priorities should they have? What is the sequence of responses triggered by a given type of event? What are the environmental side effects, and how long does it take the system to recover?

7. ACKNOWLEDGEMENTS

Financial support for field operations and laboratory analyses were provided by the four CRC institutions, the National Science Foundation and the NOAA Sea Grant Programs of the University of Maryland and the Virginia Institute of Marine Science. Vessels were provided by components of the CRC institutions as follows:

R/V Pritchard (42 feet); Chesapeake Bay Institute (CBI), The Johns Hopkins University; S. Gilbert, Captain.

R/V Aquarius (65 feet); Center for Estuarine and Environmental Study, Chesapeake Biological Laboratory (CBL), University of Maryland; M. O'Berry, Captain.

R/V Blue Fox (30-foot class); Chesapeake Bay Center for Environmental Studies (CBCES); Smithsonian Institution; Mr. Timms, Captain.

R/V Whaler (14 feet); Virginia Institute of Marine Science (VIMS); W. Mathews, J. Cumbee and S. Synder, observers.

Personnel who joined in field observations and planning sessions, included Shel Sommers from the Department of Chemistry, University of Maryland; Samuel Bird from the Department of Geology, Mary Washington College; J. Williams of the U.S. Naval Academy; Frank Fang and John Zeigler of the Virginia Institute of Marine Science.

We thank Galen Thompson for coordinating field logistics, for analyzing the suspended sediment concentrations and the sediment particle size. Monitoring stations were installed and maintained by William Hale, James Freed, Edward Rowe, David Turley and J. Van Hog. The U.S. Geological Survey kindly provided monitoring data from Remington and Fredericksburg. Field observations and support were provided by L. Joseph, L. Ruppert, A. Evans, L. Clark, E. Rosenberg and C. Lukins. Cynthia Gaskins converted rough drafts into a typed report; R. Lukens processed VIMS current data and Peggy Peoples drafted the figures.

The work of planning operations, field observations and reporting was accomplished as follows: William Cronin intercalibrated the turbidity units and compiled the hydrographic and sedimentologic data into a common format; Jack Pierce prepared and analyzed the SEM microphotographs and analyzed organic content; R. Ulanowicz made field observations and raised some important questions; B. Nelson kept field moral at a high level; G. Gross selected a target date for high inflow several months in advance; M. Nichols developed detailed plans for field observations and put the pieces into a coherent report between numerous diversionary activities; and L.E. Cronin simplified the entire study through his wisdom and editorial counsel.

This report carries the UMCEES Reference Number 81-38CBL and the VIMS SRAMSOE Number 252.

8. REFERENCES

- Allen, G.P. and P. Castaing, 1973. Suspended sediment transport from the Gironde estuary (France) onto the adjacent continental shelf. *Mar. Geol.* 14:M47-M53.
- Davis, J. (ed.), 1977. The effects of Tropical Storm Agnes on the Chesapeake Bay estuarine system. *The Ches. Res. Consort. Pub. 54*, The Johns Hopkins University Press, Baltimore, 639 pp.
- Eisma, D., J. Kalf and M. Veenhus, 1980. The formation of small particles and aggregates in the Rhine Estuary. *Neth. J. Sea Res.*, 14:172-191.
- Elliott, A.J., 1978. Observations of the meteorologically induced circulation in the Potomac estuary. *Est. and Coastal Mar. Sci.*, 6:285-299.
- Ellison, R.L. and M. Nichols, 1970. Estuarine foraminifera from the Rappahannock River, Virginia. *Contr. Cushman Found. Foram Res.* 21:1-17.
- Huggett, R., 1974. The effects of Tropical Storm Agnes on the copper and zinc budgets of the Rappahannock River. In *CRC Pub. 34*, B31-B45.
- Inglis, C. and F.H. Allen, 1957. The regimen of the Thames Estuary as affected by currents, salinities, and river flow. *Proc. Inst. Civil Engin.*, 7:827-878.
- Loder, T.C. and D.W. Hood, 1972. Distribution of organic carbon in a glacial estuary in Alaska. *Limnol. Oceanog.*, 17:349-355.
- Meade, R.H., 1972. Transport and deposition of sediments in estuaries. In: B.W. Nelson (ed.), *Environmental Framework of Coastal Plain Estuaries*. *Geol. Soc. Am. Mem.* 133:91-120.
- Meyers, P.A. and J.G. Quinn, 1973. Factors affecting the association of fatty acids with mineral particles in seawater. *Geochim. Cosmochim. Acta*, 37:1745-1759.
- National Ocean Survey, 1978. Tide tables, east coast of North America, 285 pp.
- Nelson, B.W., 1972. Biogeochemical variables in bottom sediments of the Rappahannock River estuary. In: B.W. Nelson, ed., *Environmental Framework of Coastal Plain Estuaries*, *Geol. Soc. Am. Mem.* 133:417-451.
- Nichols, M., 1977. Response and recovery of an estuary following a river flood. *Jour. Sed. Petrol.* 47:1171-1186.

- Nichols, M. and G. Poor, 1967. Sediment transport in a coastal plain estuary. Jour. Waterways and Harbors. Am. Soc. Civil Engin. 93, WW4, paper 5571; p. 83-95.
- Officer, C., 1980. Box models revisited. In: P. Hamilton, ed., Wetlands and Estuarine Processes and Water Quality Modeling. Plenum Publishing Co., N.Y., p. 65-114.
- Officer, C. and M. Nichols, 1980. Box model application to a study of suspended sediment distributions and fluxes in partially mixed estuaries. In: V. Kennedy (ed.), Estuarine Perspectives. Academic Press, N.Y., p. 329-340.
- Pearl, H.W., 1974. Bacterial uptake of dissolved organic matter in relation to detrital aggregation in marine and freshwater systems. Limnol. Oceanog., 19:966-972.
- Pierce, J.W. and F.R. Siegel, 1979. Particulate matter suspended in estuarine and oceanic waters. Scanning Electron Microscopy, /1979/I:555-562.
- Pritchard, D.W., 1969. Dispersion and flushing of pollutants in estuaries. Am. Soc. Civil Eng., J. Hydr. Divis. 95:115-124.
- Rochford, D.J., 1950. Studies in Australian estuarine hydrology. Jour. Mar. and Freshwater Research, V. 2, 116 pp.
- Schubel, J., 1977. Effects of Agnes on the suspended sediment of the Chesapeake Bay and contiguous shelf waters. In: J. Davis, ed., The Effects of Tropical Storm Agnes on the Chesapeake Bay Estuarine System. Ches. Research Consort., CRC Pub. 54, p. 179-200.
- Snedaker, S., D. deSylva and D. Cottrell, 1977. A review of the role of fresh-water in estuarine ecosystems. Final Report to the Southwest Florida Water Management District. Univ. Miami, Rosen. Sch. of Mar. and Atmos. Sci., 126 pp.
- Strickland, J.D.H. and T.R. Parsons, 1972. A practical handbook of seawater analysis. Bull. 167, Fish. Res. Bd. of Canada, Ottawa, 300 pp.
- Ulanowicz, R.E. and D.A. Flemer, 1978. A synoptic view of a coastal plain estuary. In: J. Nihoul, ed., Hydrodynamics of Estuaries and Fjords, Elsevier, Amsterdam, p. 1-26.
- U.S. Geological Survey, 1978. Water Resources Data for Virginia. U.S.G.S. Data Rept. VA-78-1, 413 pp.
- Virginia Division of Water Resources, 1970. Rappahannock River Basin, comprehensive water resources plan. V. III Hydrologic analysis. Planning Bull. 221, 176 pp.
- Zaborski, J. and D. Haven, 1980. Oyster mortalities in the upper Rappahannock River and in the Virginia tributaries of the lower Potomac. Va. Inst. of Mar. Sci. Spec. Rept. in Applied Science and Ocean Engin. 241, 12 pp.

Appendix 1. Arithmetic mean diameters (μm) of different types of particles, total sample, distribution truncated at $2.8\mu\text{m}$, and Coulter Counter (CC) data. Particle types are clean grains (CG), organic-coated grains (OG), biogenic particles (B), clean aggregates (CA), aggregates with an organic matrix (OA), and organic material only (O). From samples of April 1, 1980.

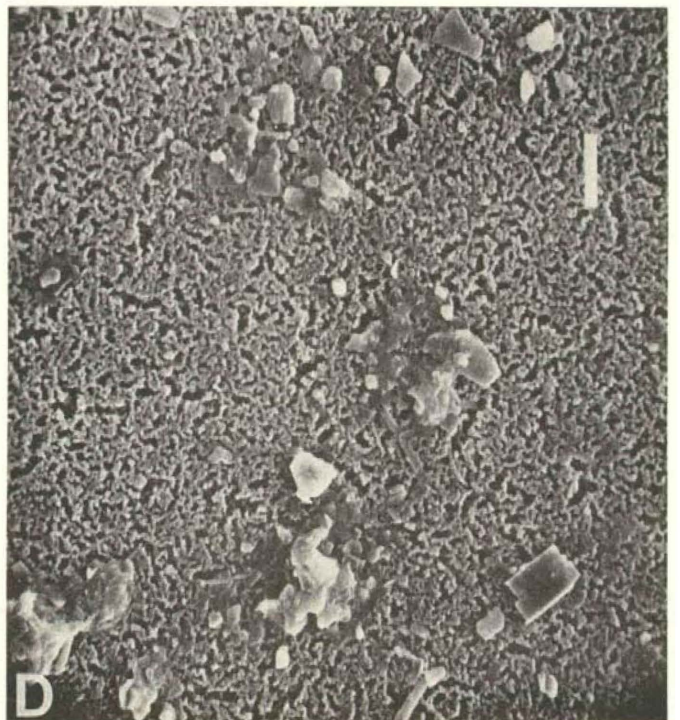
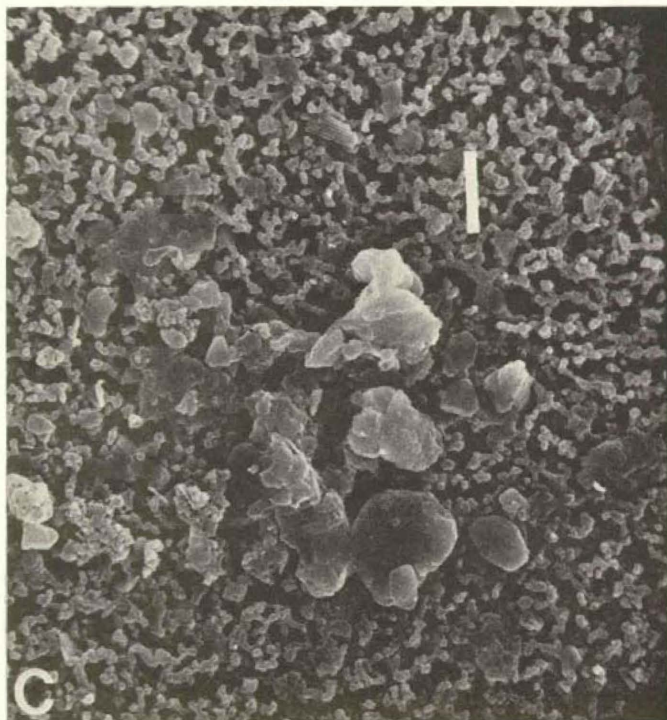
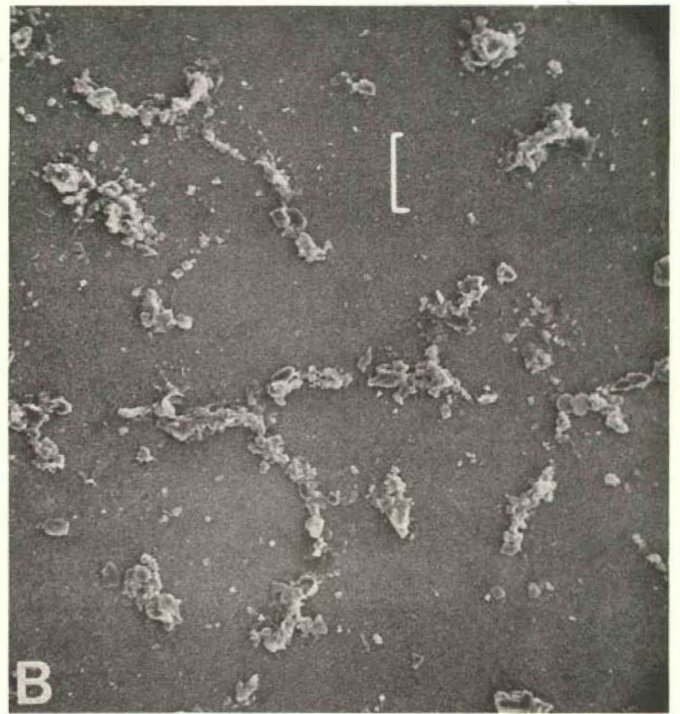
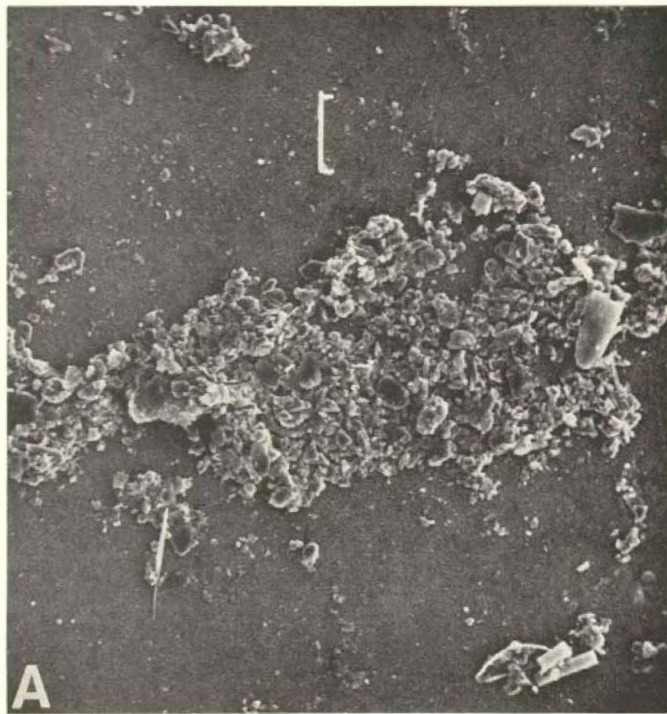
Sta/depth	CG	OG	B	CA	OA	O	total	truncated	CC
60 0	2.3	2.2	2.4	5.2	5.2	-	3.4	5.6	7.0
50 B+0.3m	1.8	4.4	18.7	25.3	34.5	-	10.0	19.2	8.9
45 0	2.5	2.5	-	5.1	6.3	5.8	4.5	6.1	6.6
B+0.3m	2.2	3.5	5.2	6.5	8.7	-	5.8	7.8	8.5
35 2	-	3.8	-	11.4	15.2	-	6.5	10.1	5.5
30 0	-	3.7	-	-	8.0	-	5.6	7.1	6.3
2	-	3.0	-	3.3	6.0	11.6	6.0	8.1	6.2
4	-	3.0	-	4.8	6.3	8.9	4.7	6.2	6.4
B+1m	4.3	2.5	5.3	4.0	5.0	4.2	4.1	5.9	5.9
B+0.3m	-	4.1	-	4.8	8.2	10.2	6.3	7.5	9.9
25 B+0.3m	5.1	2.8	4.5	5.2	14.6	6.8	7.8	10.7	7.3

Appendix 2. Model diameters (μm) from counts of particles, April 1, 1978.

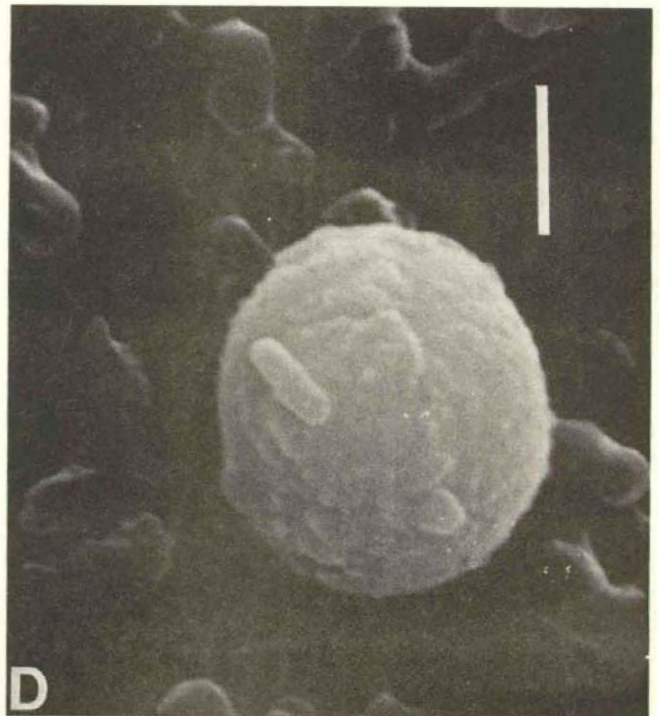
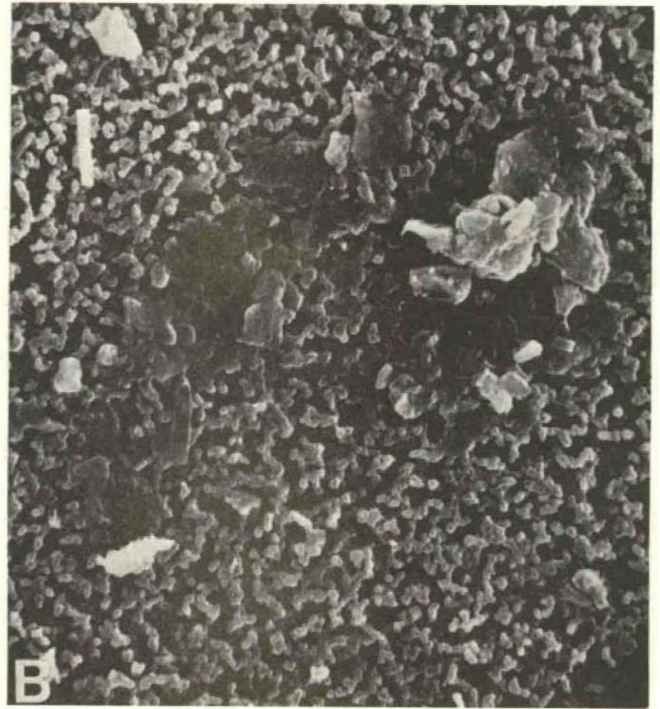
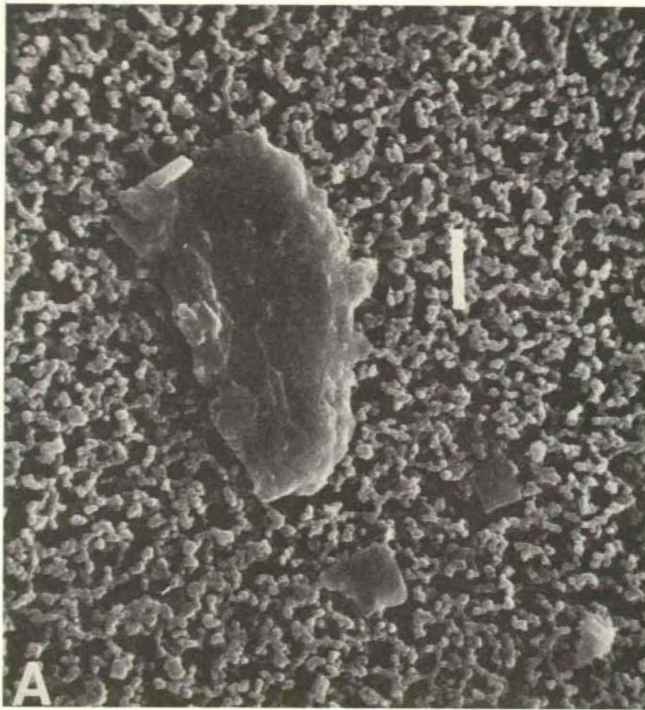
Sta.	60	50	45	35	30	25
Depth						
0	1.6		2.3		4.6	
2				3.3	2.3	
4					2.3	
B+1m					2.3	
B+0.3m		1.2	2.3		4.6	3.3

Appendix 3. Percentage of each type of particle as part of total number.

Sta/Depth	Clean Grains	Organic Coated Grains	Biota Organic Material	Clean Aggregates	Aggregates with Organic Matrix
R60 0	38.4	17.6	5.4	22.6	16.0
R50 B+0.3m	46.0	28.7	1.2	4.8	19.3
R45 B+0	3.0	41.6	5.0	2.8	47.5
B+0.3m	26.2	16.2	6.3	4.6	46.7
R35 2m	-	42.6	-	8.0	18.9
R30 0	-	43.5	-	-	56.5
2m	-	50.8	-	5.7	13.7
4m	-	60.5	-	3.7	18.4
B+1m	5.8	32.3	10.3	1.3	50.3
B+0.3m	-	54.0	-	3.5	20.2
R25 B+0.3m	2.5	45.9	9.3	3.5	38.9



Appendix 4. SEM micrographs of suspended particles. 4A and B, aggregates at R50, bar = $5\mu\text{m}$; 4D, aggregates and grains at R35, 2 m, bar = $10\mu\text{m}$. Background is surface matrix of filter.



Appendix 5. SEM micrographs of suspended particles; 5A. Single, coated grain. at R30, surface, bar = $5\mu\text{m}$; 5B. Aggregates at R30, surface, bar = $5\mu\text{m}$; 5C. Aggregate from 0.5 m above bottom, R25, bar = $10\mu\text{m}$; 5D. Small particle, approximately $1\mu\text{m}$ in diameter, which may be similar to authigenic particles reported by Eisma, et al. (1980), bar = $1\mu\text{m}$. Background is surface matrix of filter.